RESEARCH MEMORANDUM

A WIND-TUNNEL INVESTIGATION OF THE AERODYNAMIC CHARACTERISTICS OF A FULL-SCALE SUPERSONIC-TYPE THREE-BLADE PROPELLER AT MACH NUMBERS TO 0.96

By Albert J. Evans and George Liner

Langley Aeronautical Laboratory
Langley Field, Va.

NATIONAL ADVISORY COMMITTEE
FOR AERONAUTICS

WASHINGTON
July 30, 1953

NATIONAL ADVISORY COMMITTEE FOR AERONAUTICS

RESEARCH MEMORANDUM

A WIND-TUNNEL INVESTIGATION OF THE AERODYNAMIC CHARACTERISTICS OF A FULL-SCALE SUPERSONIC-TYPE THREE-BLADE PROPELLER AT MACH NUMBERS TO 0.96

By Albert J. Evans and George Liner

SUMMARY

An investigation of the characteristics of a full-scale supersonic-type propeller has been made in the Langley 16-foot transonic tunnel with the 6000-horsepower propeller dynamometer. The tests covered a range of blade angles from 20.2° to 60.2° at forward Mach numbers up to 0.96.

The results showed that envelope efficiency at an advance ratio of 2.8 decreased from 86 percent to 72 percent when the forward Mach number was increased from 0.70 to 0.96. A comparison of the experimental results with calculated results showed that maximum propeller efficiency can be calculated with good accuracy by using ordinary subsonic strip theory when the blade-section speeds are supersonic. The investigation also showed favorable power-absorption properties of the supersonic-type propeller at high speeds.

INTRODUCTION

The lack of airfoil data and adequate theory at transonic flight speeds makes the design and performance prediction of aircraft propellers uncertain for high-subsonic-speed aircraft. It is therefore necessary that the aerodynamic characteristics of propellers designed to operate at transonic speeds be determined experimentally. The experimental results not only are necessary to determine the characteristics of specific propellers but also to justify the assumptions that are necessary with respect to airfoil data and propeller theory in the transonic speed range.

Two facilities of the Langley Laboratory of the NACA, namely, the 6000-horsepower propeller dynamometer and the 16-foot transonic tunnel, have made it possible to conduct full-scale propeller tests at transonic speeds. The tests reported in this paper are the first full-scale propeller tests to be made in the transonic speed range and in a slotted wind-tunnel test section. The present investigation included measurements of thrust and torque of the propeller, wake-pressure surveys to determine the blade thrust loadings, dynamic blade twist measurements, $1 \times P$ vibratory-stress measurements, and a determination of the effects of propeller thrust on the tunnel-airspeed calibration. The present paper presents the results of the aerodynamic tests as plots of efficiency and thrust and power coefficients against propeller advance ratio for a range of forward Mach numbers from 0.20 to 0.96. The results of the tunnel airstream calibration with the 6000-horsepower propeller dynamometer installed in the test section are also included herein.

SYMBOLS

A	propeller-disk area, sq ft
b	blade width (chord), ft
C_p	power coefficient, $\frac{P}{\rho n^3 D^5}$
C_T	thrust coefficient, $\frac{T}{\rho n^2 D^4}$
C_l	section lift coefficient
D	propeller diameter, ft
h	blade-section maximum thickness, ft
J	advance ratio, $\frac{V}{nD}$
M	Mach number of advance
M_t	helical tip Mach number, $M\sqrt{1 + \left(\frac{\pi}{J}\right)^2}$

M_x	helical Mach number at station x, $M\sqrt{1 + \left(\frac{\pi x}{J}\right)^2}$
n	propeller rotational speed, rps
P	power, ft-lb/sec
P_c	power disk-loading coefficient, $\frac{P}{qAV}$
q	dynamic pressure, $\frac{1}{2}\rho V^2$
R	propeller tip radius, ft
r	radius to a blade element, ft
T	thrust, lb
V	velocity of advance, fps
x	fraction of propeller tip radius, r/R
$\beta_{0.75R}$	blade angle at 0.75R, deg
η	efficiency
ρ	air density, slugs/cu ft

APPARATUS

16-foot transonic tunnel.- The investigation was made in the Langley 16-foot transonic tunnel. The test section is octagonal in cross section with longitudinal slots permitting interference-free testing with the propeller dynamometer installed to the top speed of the tunnel as limited by the maximum power. Additional details of the wind tunnel are given in reference 1.

6000-horsepower propeller dynamometer.- The 6000-horsepower propeller dynamometer is described in reference 2. The two 3000-horsepower units of the dynamometer were coupled in tandem with the propeller mounted on the forward end for the present tests. In order to obtain a radially uniform axial flow field in the propeller plane, a long (2.4 D) cylindrical fairing extended from a point upstream of the minimum area section of the tunnel to the propeller spinner. The boundary-layer thickness in the propeller plane due to the cylindrical fairing was computed

to be of small enough magnitude to produce no noticeable effect on the operating propeller. A sketch and photograph showing the arrangement of the dynamometer and the cylindrical fairing in the tunnel are shown in figures 1 and 2, respectively.

A variable-frequency power supply allows continuous speed control of the dynamometer. The rotational speed is set manually with the aid of an aircraft tachometer and measured to within 1/4 rpm on a Stroboconn which matches rotational frequency with the known frequency of a tuning fork.

Highly refined pressure gages convert pneumatic pressures from the thrust and torque capsules into direct readings of thrust and torque. Simultaneously, spinner-juncture pressures are measured on a micromanometer to correct thrust readings for effect of air-pressure difference on the ends of the rotating spinner.

The spinner diameter was 32 inches, the same as the forward cylindrical fairing and the dynamometer case. The propeller blade airfoil sections extended inboard to the spinner surface.

Propeller.- The three-blade propeller used for this investigation was furnished by the Curtiss-Wright Corporation (design no. 109622). This propeller had a diameter of 9.75 feet. The blades were made from solid 6415 steel and had symmetrical 16-series airfoil sections. The blade-thickness ratio varied from 0.06 at the spinner to 0.02 at the tip, and the chord was constant for the length of the exposed blade. Blade-form characteristic curves are shown in figure 3. The propeller was designed to operate at a rotational speed of 2600 rpm at a forward Mach number of 0.95 at 35,000 feet altitude, corresponding to an advance ratio of 2.2.

Wake survey rakes.- The wake survey rakes were constructed so that the orifices of the total-pressure and static-pressure probes were 2 feet ahead of the leading edge of the rake strut which was an 8-percent-thick circular-arc airfoil of constant 2-foot chord. The general arrangement of the dynamometer with the wake survey rakes, mounted with the orifices located 17 inches behind the propeller center line, is shown in figures 2 and 4. Because of the difficulty of testing the propeller at high forward Mach numbers, which is explained subsequently, the rakes were set in the upper position for all but the tests at 1600 rpm.

Tests

Most of the tests were made at constant values of forward Mach number, and a range of advance ratio was covered by varying the propeller rotational speed. One group of tests was made with the propeller operating at a rotational speed of 1600 rpm to cover a complete range

of blade angles at low forward Mach numbers. For these tests, the advance ratio was varied by varying the tunnel airspeed. During the group of tests at 1600 rpm, the tunnel airspeed was lowered until flutter was audible at each blade angle tested and, although no data were recorded at flutter, the value of forward Mach number at which flutter occurred was determined.

In many cases the range of the tests was limited by the maximum dynamometer rotational speed and available dynamometer power. These limitations did not permit the testing of the propeller at its design condition of operation and also did not permit testing at low values of advance ratio at the higher Mach numbers.

Calibrations

Tunnel airspeed.- The tunnel airstream was calibrated with the dynamometer installed in the test station with no propeller. The Mach number at which the propeller tests were run was set by a Mach number indicator that was referenced to tank static pressure (16.2 ft upstream of propeller). The relationship between the Mach number at the propeller plane (without propeller) and the Mach number determined from the tank static pressure was established in the same manner as in reference 1. Evidence that propeller operation has no significant effect on tunnel wall pressures is presented in a later section of this paper.

A plot of the longitudinal Mach number distribution as measured by static-pressure orifices near the center line of one of the tunnel-wall flats and along the dynamometer body is shown in figure 1. At low speeds ($M = 0.60$), the longitudinal Mach number distribution is uniform throughout the tunnel test section. At the higher values of Mach number, however, an acceleration of the tunnel airstream is indicated in the region of the dynamometer support struts. This acceleration, which is due to the partial blockage effect of the support struts, is accompanied by a deceleration of the airstream ahead of the struts in the region of the propeller plane. The velocity gradient through the propeller plane is small, however, except at the highest value of Mach number shown.

A comparison of the results obtained from the orifices on the tunnel wall with those obtained from the dynamometer body orifices showed a negligible radial Mach number difference across the propeller plane (see fig. 1), the difference in Mach number being of the order of 0.005 at a stream Mach number of 0.95. Results from static probes of the wake survey rakes in the lower position indicated a marked difference from the results shown in figure 1. The survey rakes indicated a gradually varying radial Mach number distribution which amounted to a difference in Mach number of about 0.05 from the dynamometer to the tunnel wall at the highest value of Mach number. However, the tests made at the constant

rotational speed of 1600 rpm were the only tests made with the wake survey rakes in the lower position. The stream Mach number for the tests at 1600 rpm did not exceed a value of about 0.70, and the nonuniform radial distribution up to $M = 0.70$ is negligible.

It is believed that with the survey rakes in the lower position a partial stream blockage was caused by the proximity of the wake rake struts to the dynamometer support strut which caused the inboard static probes to record a low velocity. As shown in figure 4, the dynamometer body orifices were in the upper part of the test section, out of the area of influence of the struts, and the results did not indicate the low velocities indicated by the rake probes. In the plane of the operating propeller, the nonuniformity of the axial velocity distribution with the rakes in the lower position was further indicated by severe $1 \times P$ vibratory stresses at a Mach number of 0.70 which became worse as the Mach number was raised.

In order to overcome the above difficulties, it was necessary to move the wake survey rakes to the upper position (fig. 4). Unfortunately, there was no calibration without propeller made with the wake survey rakes in the upper position, although alleviation of the blockage effect was indicated by the absence of $1 \times P$ vibration on the operating propeller even to the maximum speed of the tunnel.

With the wake survey rakes in the upper position, the radial Mach distribution was therefore presumed to agree with the results indicated by figure 1. From the foregoing considerations, it has been concluded that the propeller data presented in the present paper do not include any detrimental effects that may be considered to arise from propeller operation in a nonuniform airstream and that the values of stream Mach number obtained from the tunnel-wall orifices are the values experienced by the operating propeller.

Dynamometer calibration.- Static calibrations of the thrust and torque meters were made in a manner similar to that for the 2000-horsepower propeller dynamometer described in reference 3. The calibrations were straight lines when the indicated loads were plotted against the applied loads and the slopes of the lines were determined by the method of least squares.

The probable error in the thrust scale readings was 5.6 pounds which amounted to a maximum error of about 0.6 percent in the important operating range of the propeller. The probable error in the total torque readings was 4.9 foot-pounds which was a maximum error of about 0.3 percent in the range of propeller operation for peak efficiency.

Reduction of Data

Thrust.- Propeller thrust as used in this report is defined as the shaft tension produced by the aerodynamic forces acting on the propeller blades from the spinner to the blade tips.

The aerodynamic forces on the rotating spinner were determined by running the tunnel and the dynamometer over a range of airspeed and rotational speed with no propeller installed and recording the readings of the thrust scales. The difference in pressure between the upstream face and the downstream face of the rotating spinner was recorded simultaneously with the thrust readings. The variation of thrust with the spinner-juncture pressure difference was one straight line for all combinations of tunnel airspeed and dynamometer rotational speed. With this relation determined, the spinner-juncture pressure difference was measured for test points with the propeller operating and the corresponding value of thrust was subtracted from the indicated scale readings as a tare thrust. Propeller thrust is, therefore, the indicated thrust of the propeller minus the spinner tare thrust created by the difference in spinner-juncture pressure between the upstream and downstream faces of the spinner, the spinner skin-friction drag being less than the accuracy of the thrust readings.

Torque.- Torque tare readings were obtained simultaneously with the thrust tare readings during the tare runs. The torque tare forces varied with tunnel airspeed and to a slight extent with dynamometer rotational speed. The variation with rotational speed amounted to about 5 foot-pounds for the range of rotational speeds presented herein. The variation of torque with tunnel airspeed, however, was a straight-line variation which amounted to about 55 foot-pounds at a value of Mach number of 1.0. Inherent vibration of the dynamometer with the wind tunnel was believed to cause the variation of torque with tunnel airspeed.

The torque tare forces for all rotational speeds were plotted against a function of tunnel airspeed and a faired line was drawn through the points. This procedure neglected the small variation of torque with rotational speed so that there was an error of $\pm 2\frac{1}{2}$ foot-pounds. Propeller torque was the indicated torque reading minus the torque tare readings.

Wind-tunnel wall correction.- A theory was presented in reference 4 for the solid blockage interference effect in circular wind tunnels with walls slotted in the direction of flow. The theory indicated the possibility of obtaining zero blockage interference at high subsonic Mach numbers, and tests on a model tunnel reported in the same reference confirmed the theoretical results. Pressure measurements on a body of revolution in the Langley 16-foot transonic tunnel are compared with

measurements made on an identical body by the free-fall technique in reference 5. The results of reference 5 showed that the tunnel-wall interference effects were negligible up to and including Mach number 1.0.

In order to check the wall effect of a slotted test section on an operating propeller, pressure measurements were made along a region of the wind-tunnel wall extending from 1.3 feet ahead to 4.2 feet behind the propeller plane. The results of the pressure measurements are presented in figure 5 as the variation with tunnel station of the ratio of the Mach number with the propeller operating to the Mach number obtained from calibration tests without a propeller. The shaded area between the two curves includes representative data obtained throughout the entire Mach number and propeller-thrust-coefficient ranges covered in the investigation. The scatter of points in the enclosed area of figure 5 is within the accuracy of the tunnel speed measurements. The Mach number with the propeller operating was within about ±1.0 percent of the values obtained without the propeller, and the tunnel longitudinal Mach number gradient with the propeller operating was essentially the same as that obtained without the propeller (fig. 1). The variation of thrust coefficients from a negative value to a relatively high positive value did not appreciably affect the Mach number ratio. Since it is evident that the operating propeller had no significant effect on the tunnel wall pressures, it has been concluded that no wind-tunnel wall correction is necessary for the ranges of Mach number and thrust coefficient covered in the present tests.

Accuracy.- In the significant range of propeller operation the data are accurate to 1.3 percent based on the accuracy of the static calibrations. However, the accuracy of the faired curves is believed to be within 1.0 percent.

RESULTS AND DISCUSSION

Presentation of basic results.- The aerodynamic data obtained during the tests are presented in figures 6 to 14 as faired curves of thrust coefficient, power coefficient, propeller efficiency, airstream Mach number, and helical-tip Mach number plotted against propeller advance ratio. The data test points are included on the plots of thrust and power coefficients.

Many of the tests were extended into the negative thrust and power range of operation and the data have been included in figures 6 to 14. The curves indicate that data obtained in the positive range of operation can be extrapolated to small negative values with good accuracy.

The plot of thrust coefficient and efficiency in figure 14 for $\beta_{0.75R} = 54.7^{\circ}$ was obtained from wake survey pressure data since the thrust data obtained for this particular test were believed to be erroneous because of difficulties which were encountered in the operation of the thrust capsule.

In some cases the data have been extrapolated to define the efficiency peaks better. The extrapolated portions of the curves are shown in the figures as a dashed line. The values of peak efficiency obtained by extrapolation are considered to be within the experimental accuracy of the data.

Discontinuities in some of the Mach number curves shown in figures 6 to 14 were caused by changes in air temperature which occurred from day to day.

The effects of advance ratio on envelope efficiency.- Figure 15 shows the variation of envelope efficiency with advance ratio for several values of forward Mach number. The most notable feature of the curves in figure 15 is that the loss in efficiency with an increase in advance ratio is small for any of the Mach numbers. Although the design value of advance ratio (2.2) could not be reached at the higher Mach numbers, the trend of the curves indicates that a supersonic propeller designed for an advance ratio of 2.2 will experience a loss in envelope efficiency of only about 1 percent when operated at an advance ratio of 3.2. As advance ratio is increased above 3.2 the drop in envelope efficiency is more rapid. The curves in figure 15 suggest the possibility that a supersonic propeller could be designed for advance ratios as high as 3.4. At these higher advance ratios the rotational speed would be much lower, and the structural problem caused by large centrifugal forces would be less severe; therefore, thinner blade sections might be used. Although there is an increase in the tendency to flutter, the use of thinner blade sections would be a definite advantage because of their higher lift-drag ratios at high Mach numbers. However, the use of a lower rotational speed would lower the power-absorption properties of the propeller with a given diameter, since the power varies as the cube of the rotational speed. Obviously, the selection of the proper advance ratio for a supersonic propeller involves a compromise between aerodynamic and structural requirements.

Comparison of calculated and experimental values of envelope efficiency.- It was not possible to test the present propeller at the design operating conditions since the maximum rotational speed of the dynamometer (2300 rpm) did not permit operation at a V/nD of 2.2 at a forward Mach number of 0.95. Strip theory calculations, however, have been made for the efficiency of the propeller by using the method described in reference 3 and the results are plotted in figure 15. The airfoil data

which were cross-plotted and extrapolated for use with the blade-thickness ratios of the test propeller, were obtained for the calculations from reference 6.

On the basis of the calculated values of efficiency being nearly constant between a J of 2.20 and 2.86, the experimental curve for a Mach number of 0.96 is faired to $J = 2.2$ as shown in figure 15. This extrapolation of the experimental curve indicates an efficiency of the test propeller for $M = 0.96$, $J = 2.20$ of about 73 percent. There is remarkably close agreement shown with the calculated values of efficiency for this propeller compared to the experimental data in figure 15. In the worst case ($J = 3.78$) the difference between the calculated efficiency and experimental efficiency is 0.025, whereas at $J = 2.86$ the difference is 0.008. For the calculations at $J = 3.78$, some of the effective blade sections were operating in a transonic speed range where a small error of Mach number or angle of attack might result in a large error in drag. The agreement at the lower advance ratio shows that, when the blade section speeds are supersonic, maximum propeller efficiency can be calculated with good accuracy by using ordinary subsonic strip theory and the airfoil data compiled in reference 6. The calculations of thrust and torque coefficients, however, were about 20 percent below the experimental values. This result indicates that the lift-drag ratios used in the calculations were satisfactory but the values of both lift and drag were somewhat low.

Effect of forward Mach number on maximum efficiency.- The variation of maximum propeller efficiency with forward Mach number is shown in figure 16 for advance-ratio values of 2.8, 3.4, and 4.0. These data show that the maximum efficiency attained during the tests was 86 percent between Mach numbers of 0.60 and 0.70 at an advance ratio of 2.8. Above $M = 0.70$, the efficiency decreased gradually to a value of 72 percent at the Mach number of 0.96. At an advance ratio of 4.0, the maximum efficiency was 2.5 to 4.0 percent less than that for $J = 2.8$ over the Mach number range from 0.60 to 0.96.

Results of this investigation of the supersonic propeller agree with trends shown for model propellers designed for higher advance ratios (ref. 7) than 2.2. At a constant value of forward Mach number any increase in advance ratio decreases rotational speed and therefore results in lower values of blade section Mach number. It is thus apparent that a propeller operating at high J will delay the onset of the adverse effects of compressibility on the blade sections and will operate to higher values of forward Mach number before the blade sections reach the critical speed. It is seen in figure 16 that the critical speed of the test propeller was delayed to higher Mach numbers as advance ratio was increased. At $J = 2.8$ the point at which the efficiency began to decrease rapidly was $M = 0.71$ and progressed to $M = 0.75$ at $J = 3.4$ and $M = 0.80$ at $J = 4.0$. Furthermore, as the value of

forward Mach number is increased into the supercritical speed range, the present propeller and the model propellers of reference 7 will operate at a low J more efficiently than at a high J because of the more advantageous orientation of the blade force vectors.

Below the critical Mach number, there is a notable difference of the advance ratio at which maximum efficiency is attained between the model propeller of reference 7 and the propeller of this paper. Obviously, the model propeller operating at advance ratios lower than the design value of 3.36 will not have all blade sections at maximum L/D resulting in a lower efficiency. The present propeller will operate with efficiency decreasing as advance ratio is increased away from the design value of 2.2 for the same reason.

Power coefficient for maximum efficiency.- The variation of power coefficient for maximum efficiency with advance ratio is shown in figure 17 for constant values of forward Mach number. These curves can be used to evaluate the power-absorption properties of the low J, supersonic-type propeller. If a constant pressure altitude and a constant Mach number of 0.96 is assumed, the propeller operating at an advance ratio of 2.8 would absorb nearly twice as much power and, as shown in figure 15, would operate 3 percent more efficiently than a similar propeller operating at an advance ratio of 3.8. More power is absorbed when operating at the lower advance ratio because the power absorbed is inversely proportional to advance ratio, although the power coefficient is lower at the lower advance ratio. Another way to illustrate the advantages of operation at low advance ratios is to compare the diameters of propellers designed for a given power. In the foregoing example, the propeller operating at an advance ratio of 3.8 would have to be 40 percent greater in diameter to absorb the same power as the propeller operating at an advance ratio of 2.8. Therefore, the supersonic-type propeller with low design advance ratio has favorable power-absorption characteristics which permit the use of smaller propeller diameters.

Comparison of data with compressible momentum theory.- A compressible momentum theory has been developed in reference 8, some results of which are reproduced in figure 18. Values of maximum efficiency obtained experimentally in the present tests are also plotted as data points in figure 18.

The compressible momentum theory based on the assumption of a subsonic slipstream indicates that, as the propeller power disk loading is increased beyond a certain value at a constant forward Mach number, the ideal efficiency decreases very rapidly and, if such were the case in practice, would preclude the use of propellers at Mach numbers above about 0.90. As pointed out in reference 8, however, the propeller slipstream can attain supersonic speeds when the power is increased, and the values of efficiency shown in figure 18 for the supersonic wake appear

to be more reasonable. Although the calculated values of efficiency in figure 18 do not include any profile or rotational losses, most of the experimental data for the higher Mach numbers (0.93 and 0.96) are above the subsonic-wake curves. It appears, therefore, that the propeller slipstream must have attained supersonic velocities for at least a short distance behind the propeller for the tests at $M = 0.93$ and $M = 0.96$.

Operating charts.- In order to facilitate the use of the data included herein for performance estimates, charts have been prepared and are included in figure 19. The charts consist of plots of power coefficient against advance ratio with lines of constant efficiency superimposed. The charts are presented for the constant values of forward Mach number tested and one chart presents the data obtained at a constant value of rotational speed of 1600 rpm (for $M < 0.67$).

Stall-flutter data.- The purpose of the present investigation was to determine the aerodynamic characteristics of the subject propeller, and the propeller was not deliberately run at flutter since violent or sustained flutter would have been hazardous to the test equipment. Flutter was detected, however, both audibly and by strain gages during the constant rotational speed tests at 1600 rpm when propeller stall conditions were encountered. In some cases it was possible to record the value of forward Mach number at flutter whereas in other cases the dynamometer speed was dropped slightly before data were taken.

No analysis of the flutter data is presented, but the data obtained are included in figure 6. The values of advance ratio at which flutter occurred were spotted on the curves of thrust and power coefficient and a curve drawn through the points to mark the flutter boundary.

The flutter data, as replotted in figure 20, show the variation of the section lift coefficient at flutter with advance ratio for the $x = 0.60$ station as determined from wake pressure measurements. The values are shown for the $x = 0.60$ station since the maximum value of lift coefficient along the propeller-blade radius occurred at approximately this station.

Effect of strain gages on propeller efficiency.- Most of the tests for this report were run with strain gages cemented to the surface of one of the propeller blades. Consideration of the effect of the strain gages on the aerodynamic characteristics led to the repeat tests with the strain gages removed from the propeller; thus, the propeller was aerodynamically clean. Data shown in figure 21 gave indication of no difference in maximum efficiency up to a Mach number of 0.88. Above $M = 0.88$, the clean blades were a little more efficient (about 2 percent at $M = 0.96$) than the gaged blades.

It should be noted that the aerodynamic characteristics presented in this report at high Mach numbers were obtained with the clean propeller. At values of Mach number below 0.90, the differences in efficiency between the gaged propeller and the clean propeller were negligible.

CONCLUSIONS

Tests of a supersonic three-blade propeller have been made on the 6000-horsepower propeller dynamometer in the Langley 16-foot transonic tunnel over a range of blade angles at forward Mach numbers up to 0.96. The results of the investigation indicate the following conclusions:

1. In the range of the tests the tunnel-wall interference was found to be negligible for propeller operation in the slotted test section of the Langley 16-foot transonic tunnel.

2. Envelope efficiency at an advance ratio of 2.8 decreased from 86 percent to 72 percent when the forward Mach number was increased from 0.70 to 0.96.

3. Maximum propeller efficiency can be calculated with good accuracy by using ordinary subsonic strip theory when the blade-section speeds are supersonic.

4. The loss in envelope efficiency with increase in advance ratio is only about 1 percent between advance ratios of 2.2 and 3.2.

5. The supersonic-type propeller with a low design advance ratio has favorable power absorption characteristics which permit the use of smaller propeller diameters.

6. A comparison of the experimental data with compressible momentum theory indicates that the propeller slipstream attained supersonic velocities for at least a short distance behind the propeller at forward Mach numbers of 0.93 and 0.96.

Langley Aeronautical Laboratory,
National Advisory Committee for Aeronautics,
Langley Field, Va., May 18, 1953.

REFERENCES

1. Ward, Vernon G., Whitcomb, Charles F., and Pearson, Merwin D.: Air-Flow and Power Characteristics of the Langley 16-Foot Transonic Tunnel with Slotted Test Section. NACA RM L52E01, 1952.

2. Wood, John H., and Swihart, John M.: The Effect of Blade Section Camber on the Static Characteristics of Three NACA Propellers. NACA RM L51L28, 1952.

3. Corson, Blake W., Jr., and Maynard, Julian D.: The Langley 2000-Horsepower Propeller Dynamometer and Tests at High Speed of an NACA 10-(3)(08)-03 Two-Blade Propeller. NACA TN 2859, 1952.

4. Wright, Ray H., and Ward, Vernon G.: NACA Transonic Wind-Tunnel Test Sections. NACA RM L8J06, 1948.

5. Hallissy, Joseph M., Jr.: Pressure Measurements on a Body of Revolution in the Langley 16-Foot Transonic Tunnel and a Comparison with Free-Fall Data. NACA RM L51L07a, 1952.

6. Anon.: Propeller Performance Analysis. Aerodynamic Characteristics. NACA 16 Series Airfoils. Rep. No. C2000, Curtiss-Wright Corp., Propeller Div. (Caldwell, N. J.), Dec. 2, 1948.

7. Delano, James B., and Carmel, Melvin M.: Investigation of the NACA 4-(0)(03)-045 and NACA 4-(0)(08)-045 Two-Blade Propellers at Forward Mach Numbers to 0.925. NACA RM L9L06a, 1950.

8. Delano, James B., and Crigler, John L.: Compressible Flow. Solutions for the Actuator Disk. NACA RM L53A07, 1953.

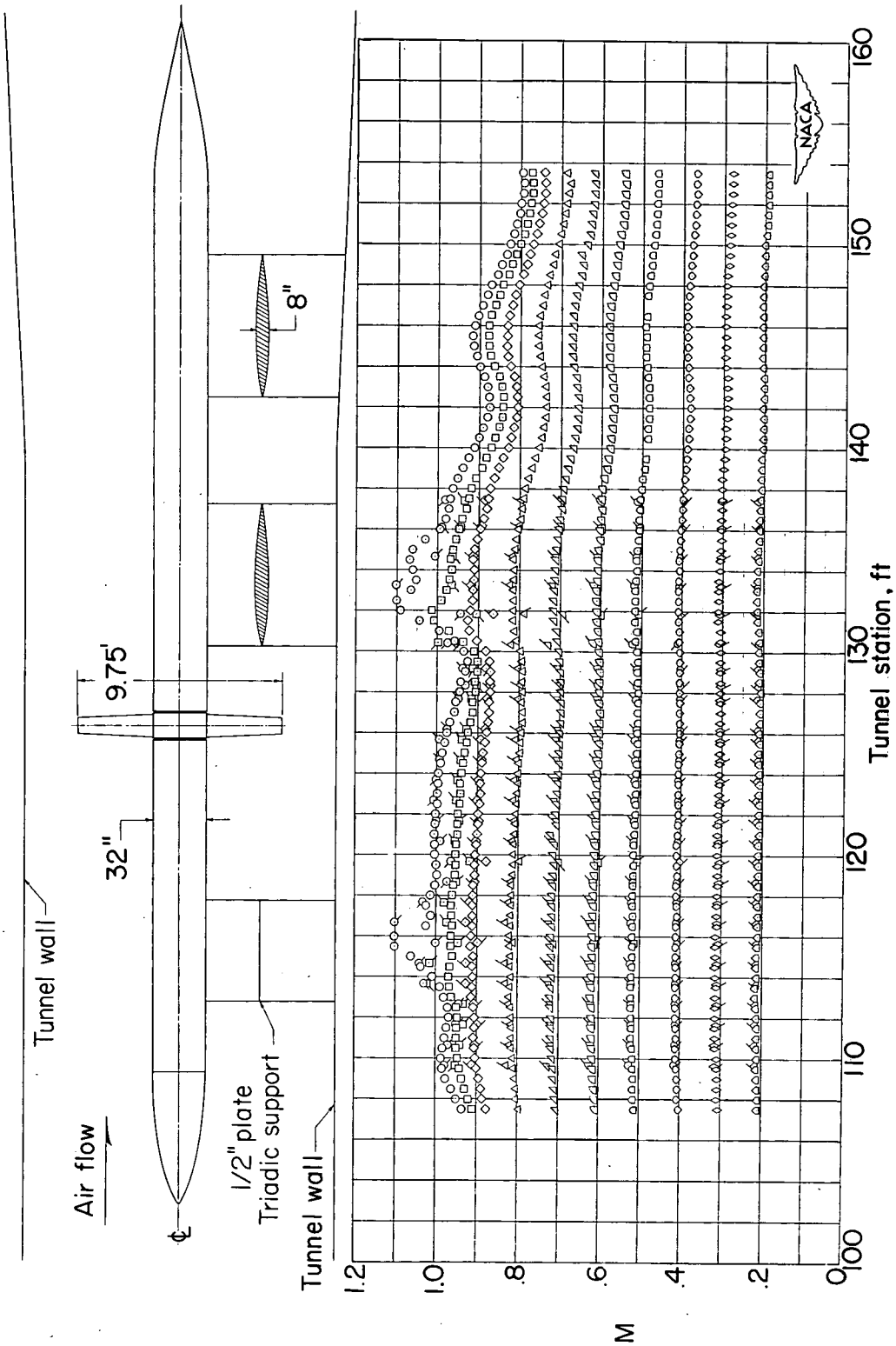

Figure 1.- Sketch of propeller dynamometer and Mach number distributions in the Langley 16-foot transonic tunnel with dynamometer but without propeller installed. Flagged symbols indicate dynamometer body measurements whereas symbols without flags represent tunnel wall measurements.

Figure 2.- Propeller mounted on the 6000-horsepower dynamometer in the Langley 16-foot transonic tunnel test section (tunnel open, view looking downstream).

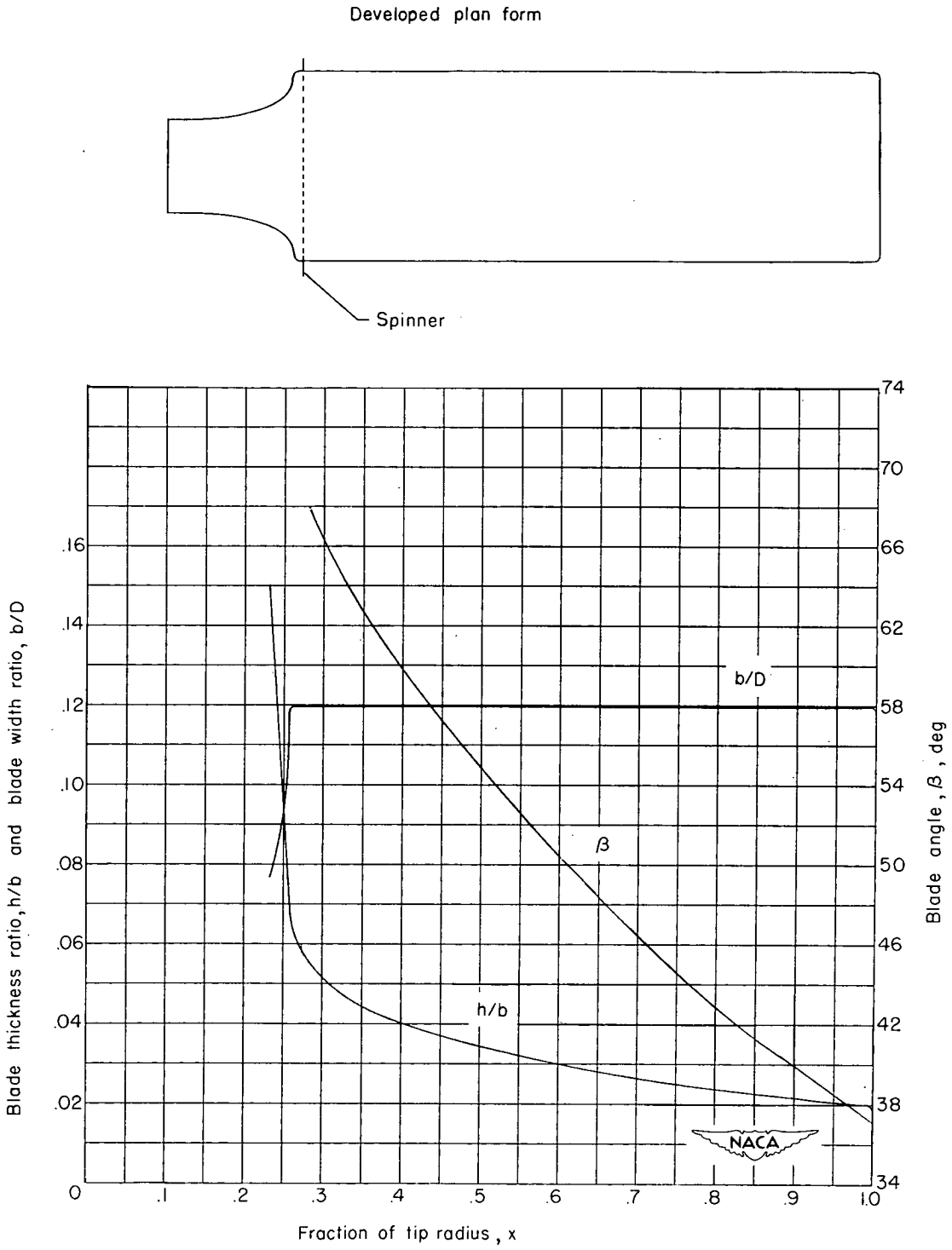

Figure 3.- Blade-form characteristics.

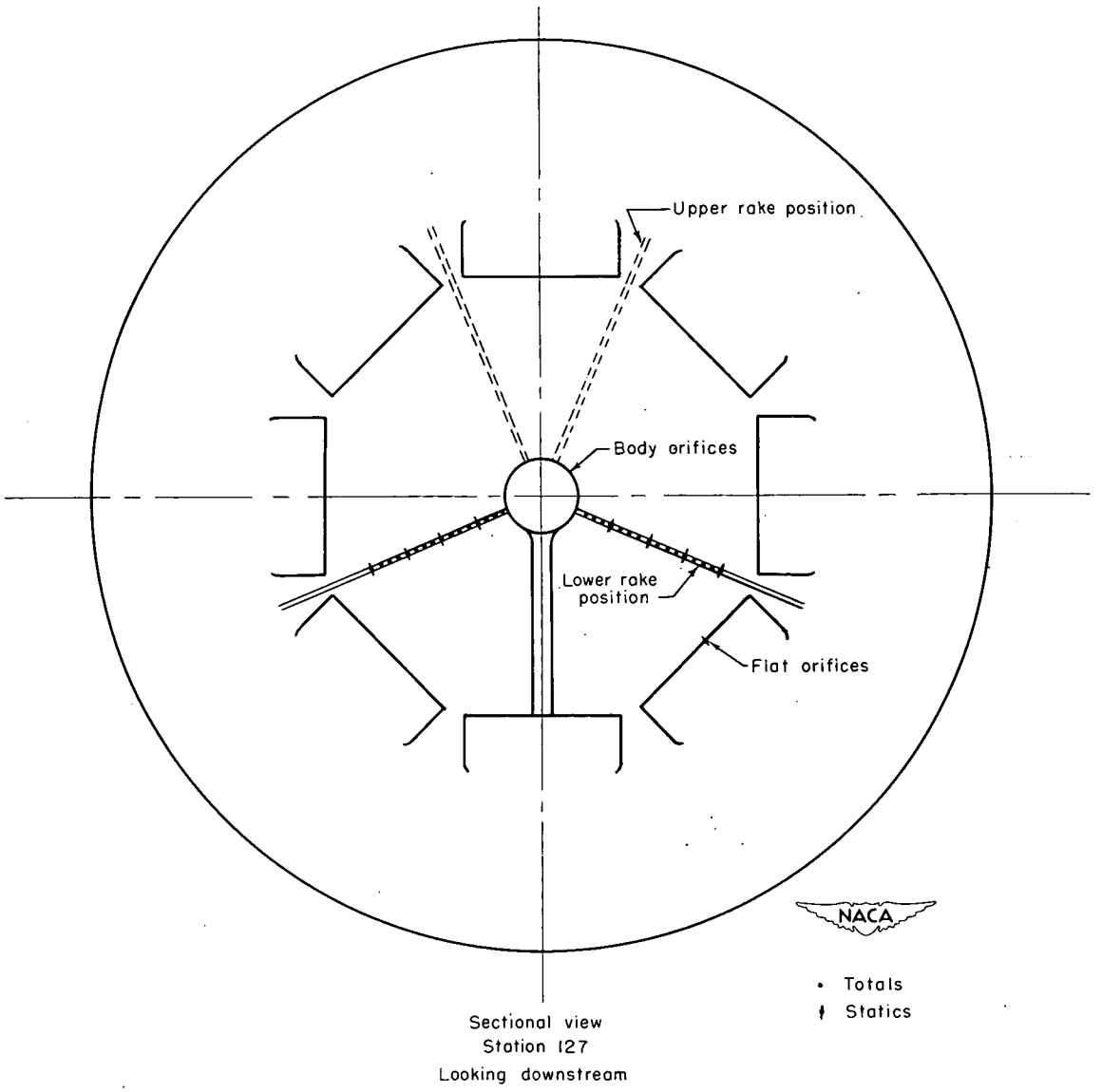

Figure 4.- Schematic diagram of dynamometer and survey rakes mounted in the test section.

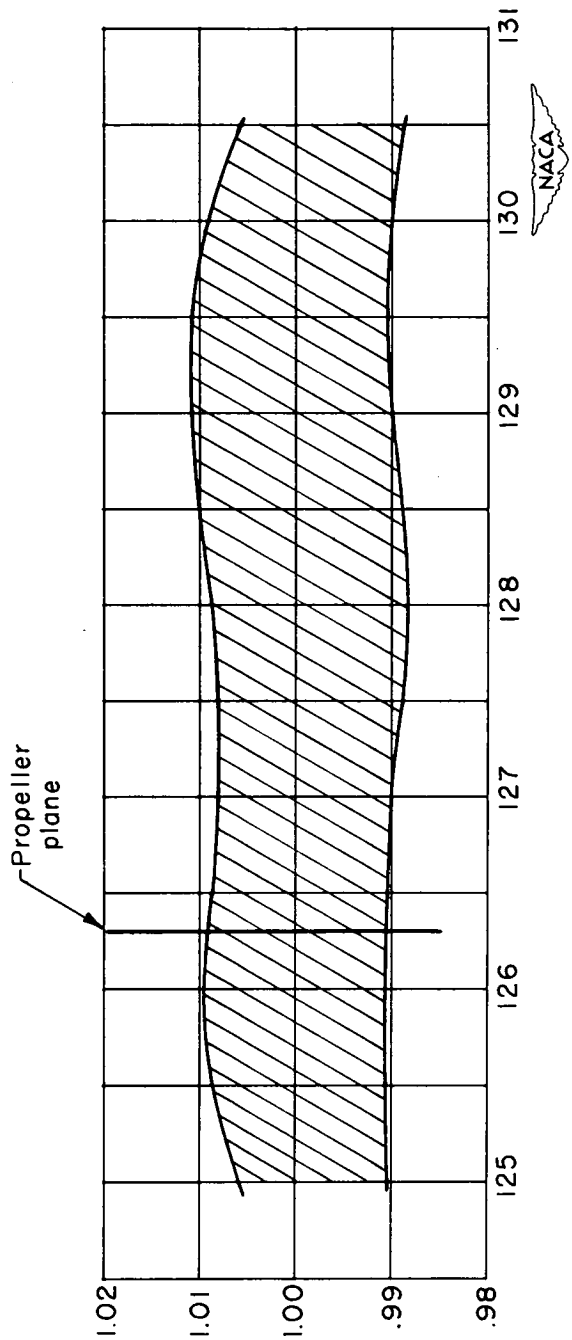

Figure 5.- Effect of propeller operation on the tunnel-wall measurements for the range of Mach numbers and thrust coefficients obtained in the tests.

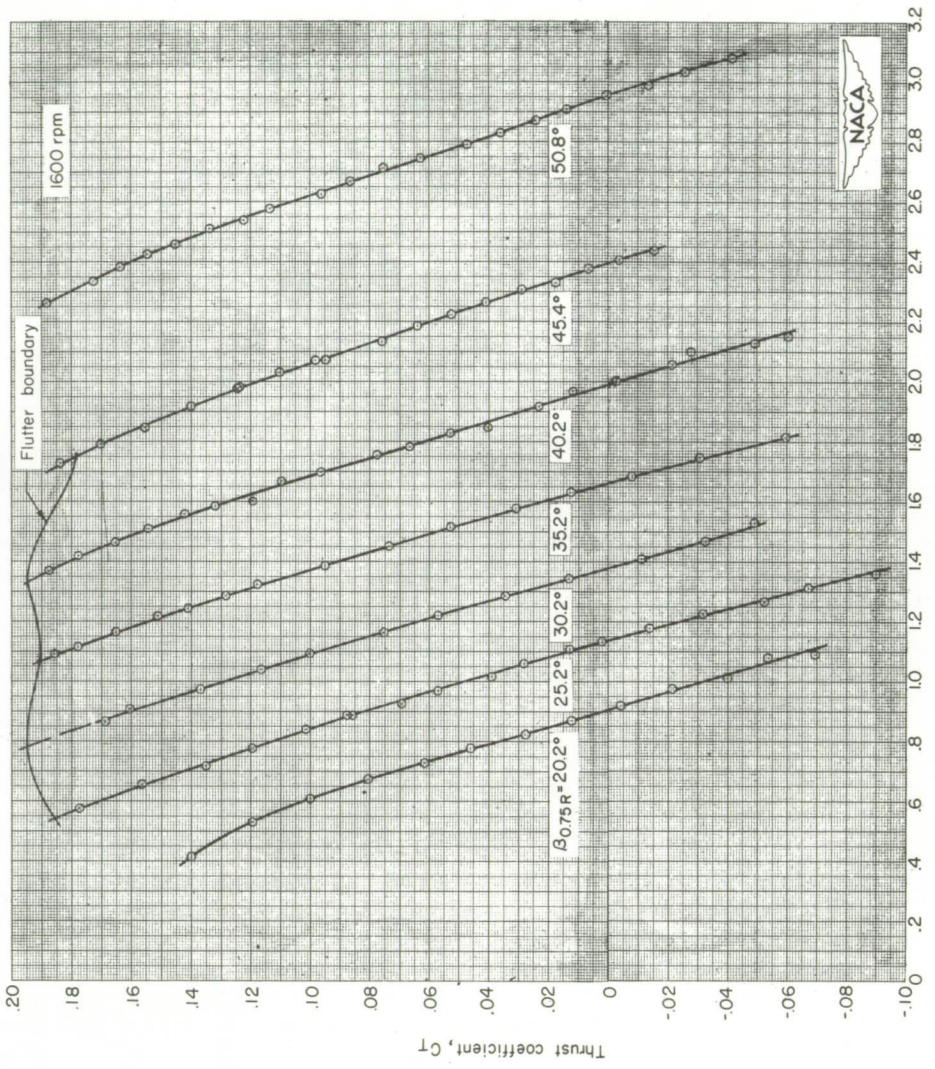

(a) Thrust coefficient.

Figure 6.- Characteristics of propeller. Rotational speed 1600 rpm; $M < 0.67$.

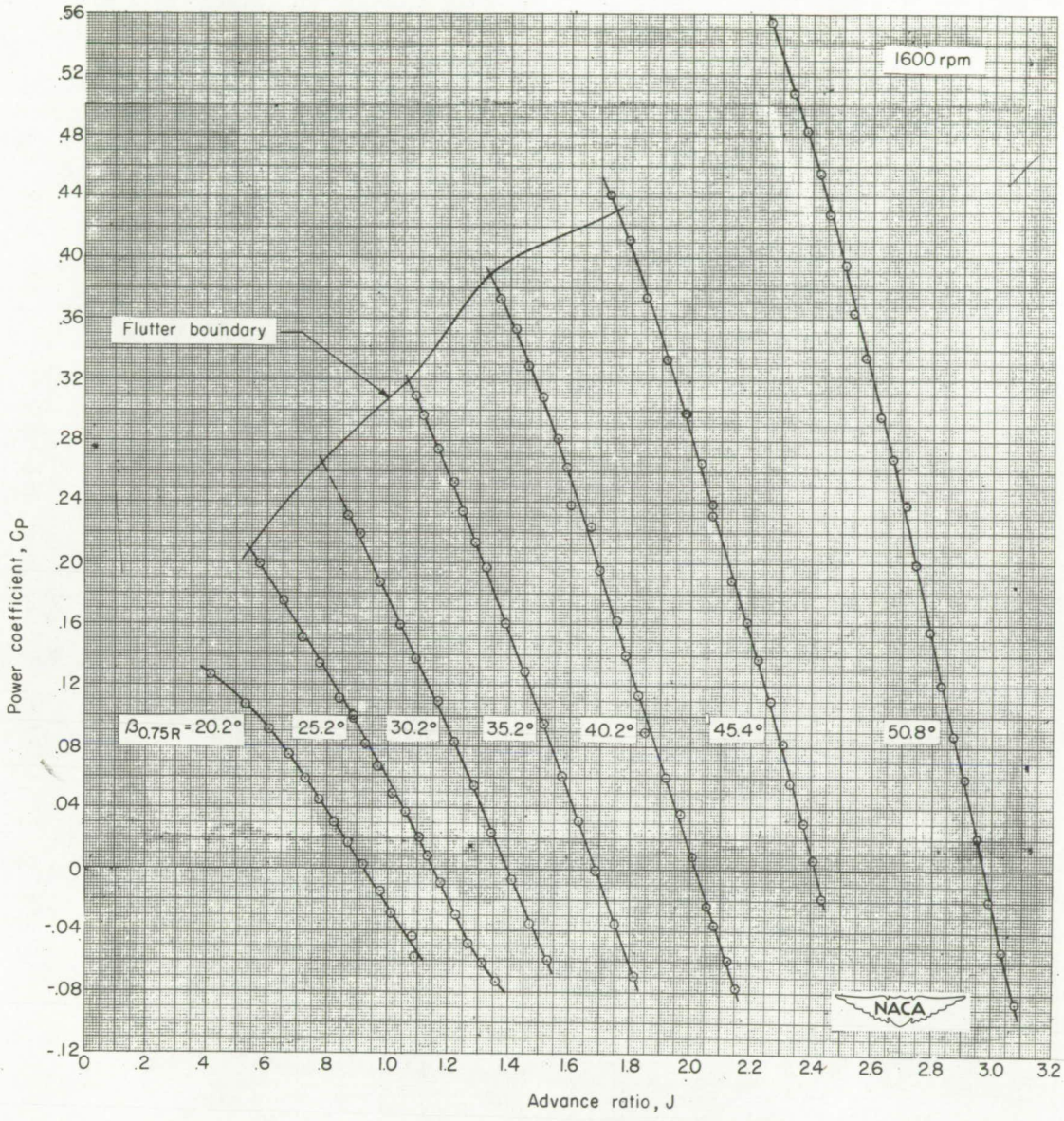

(b) Power coefficient.

Figure 6.- Continued.

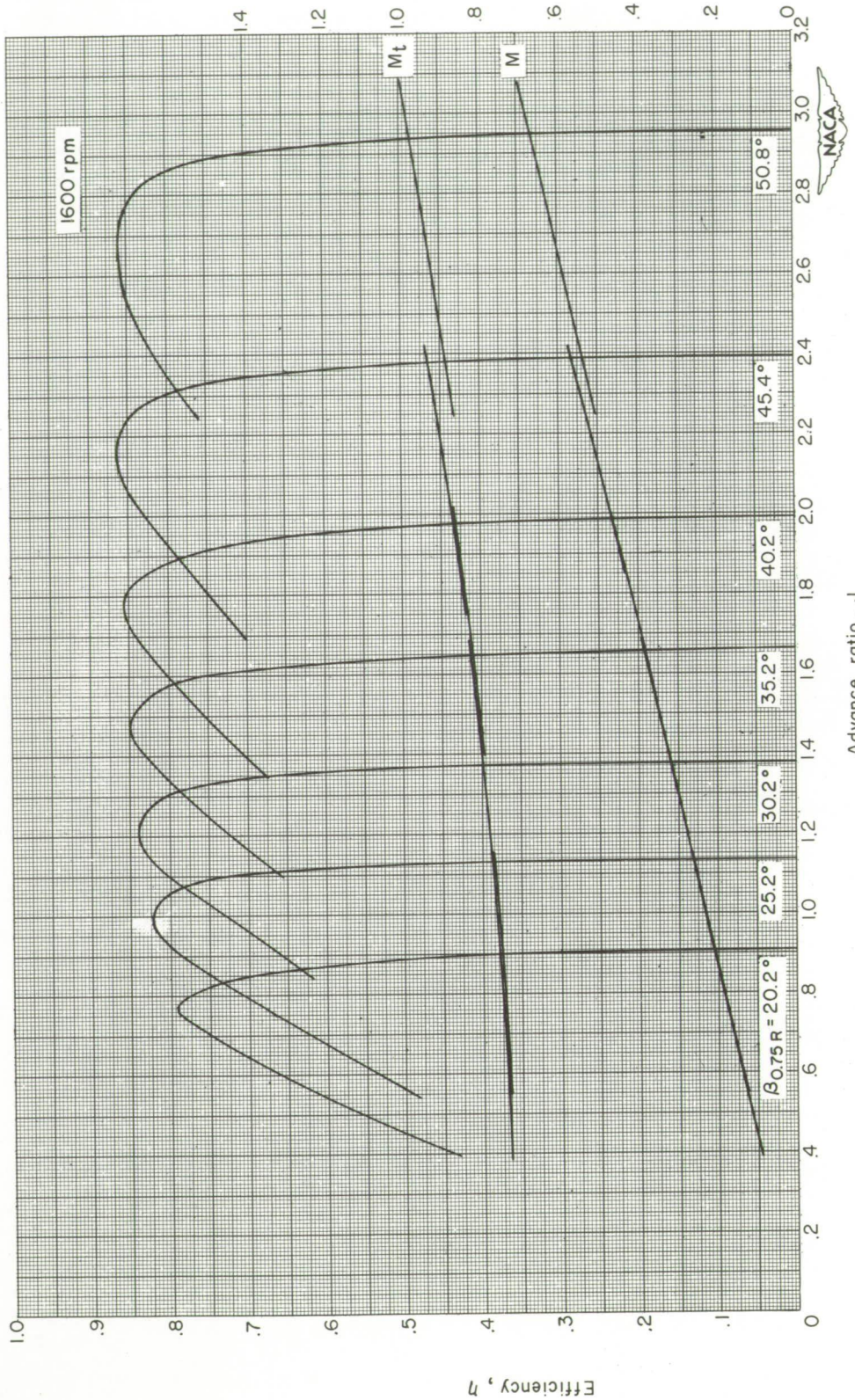

(c) Efficiency.

Figure 6.- Concluded.

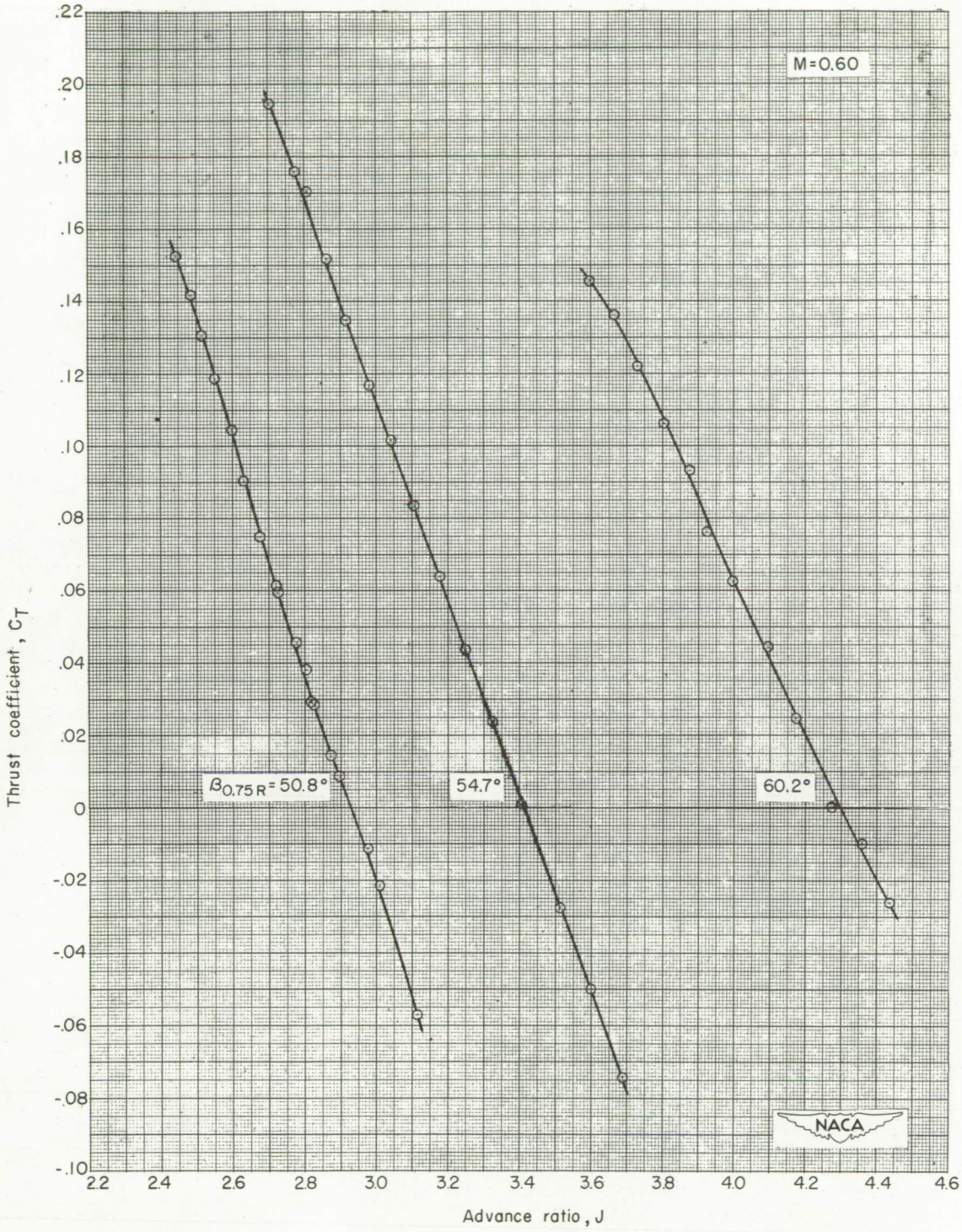

(a) Thrust coefficient.

Figure 7.- Characteristics of propeller. Forward Mach number 0.60.

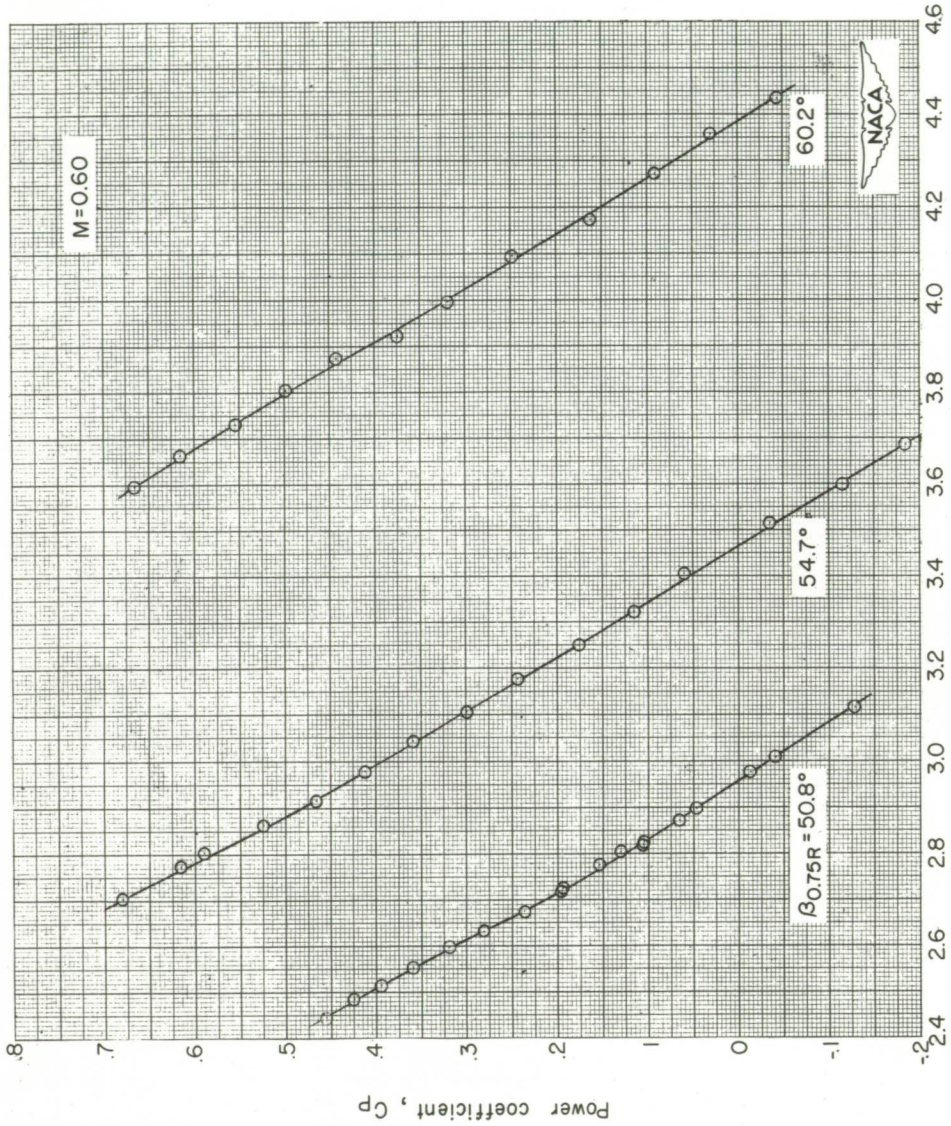

(b) Power coefficient.

Figure 7.- Continued.

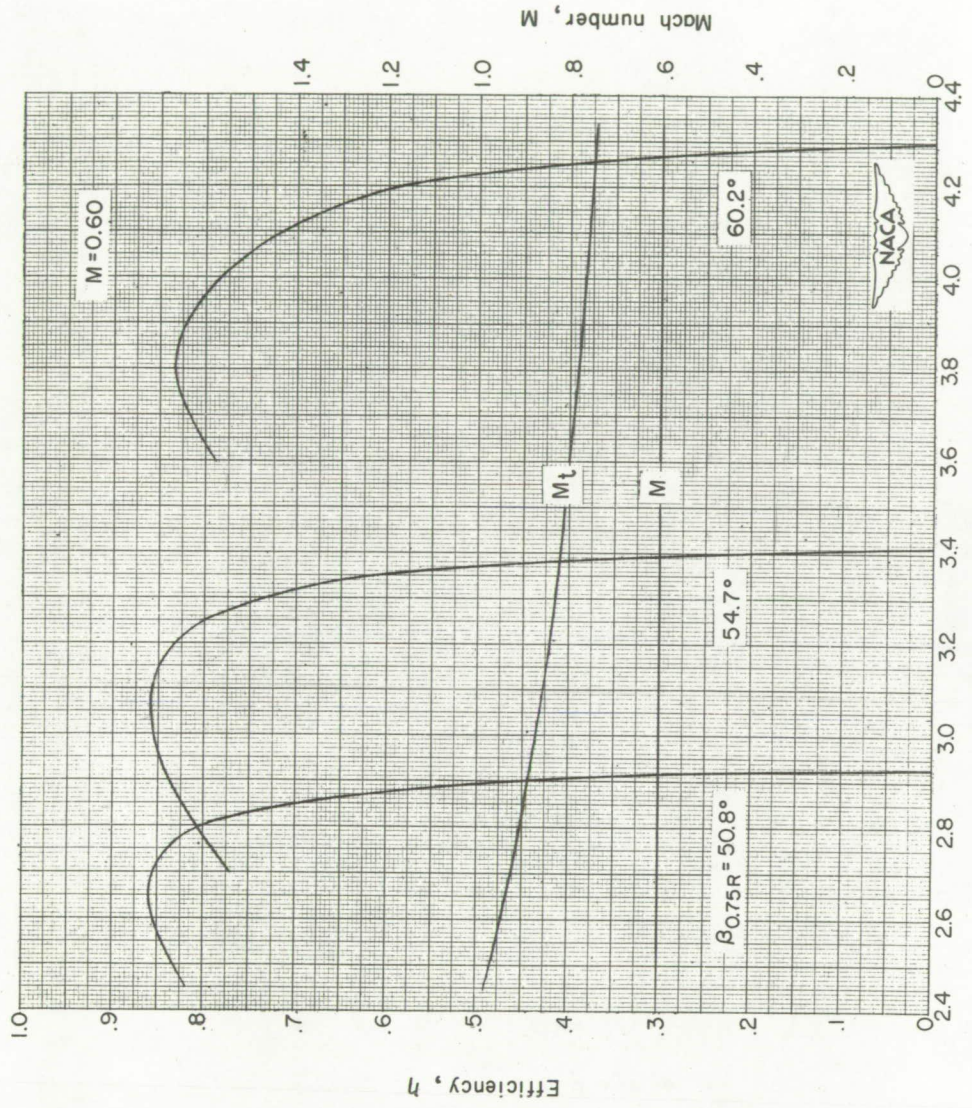

(c) Efficiency.

Figure 7.- Concluded.

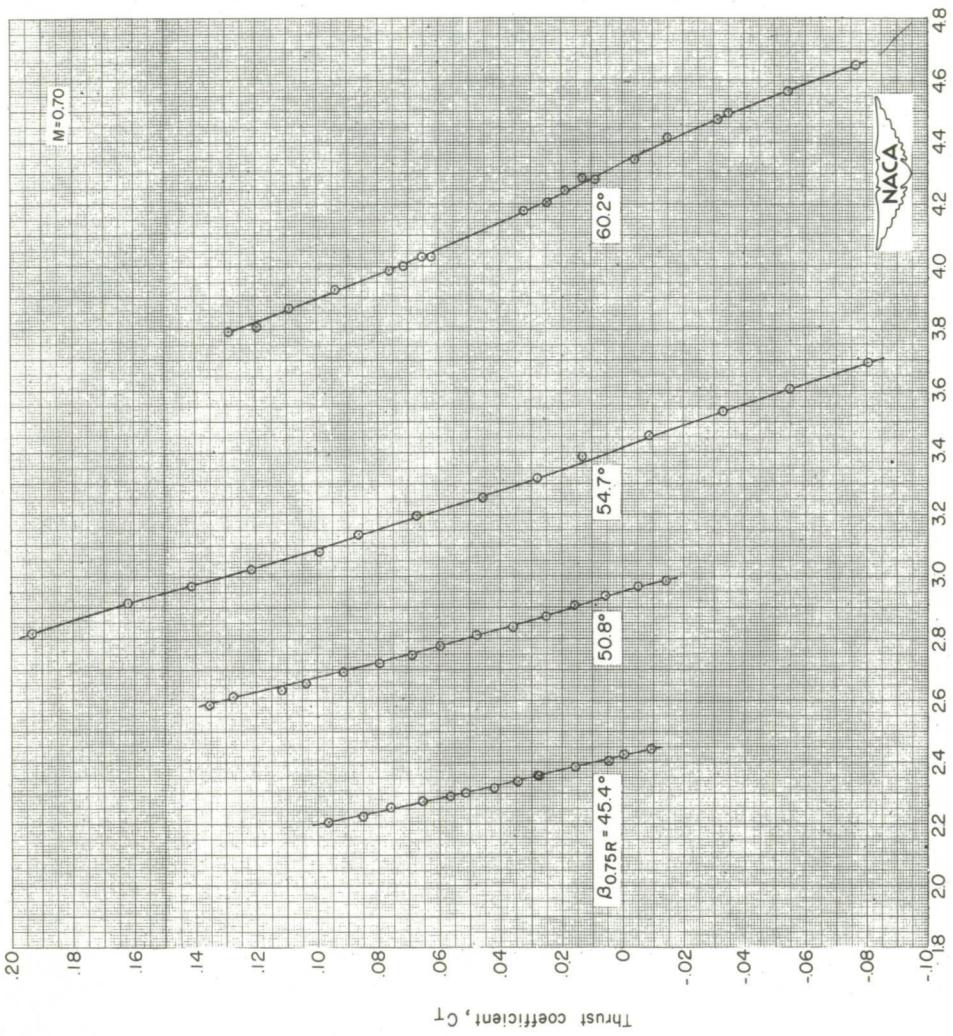

(a) Thrust coefficient.

Figure 8.- Characteristics of propeller. Forward Mach number 0.70.

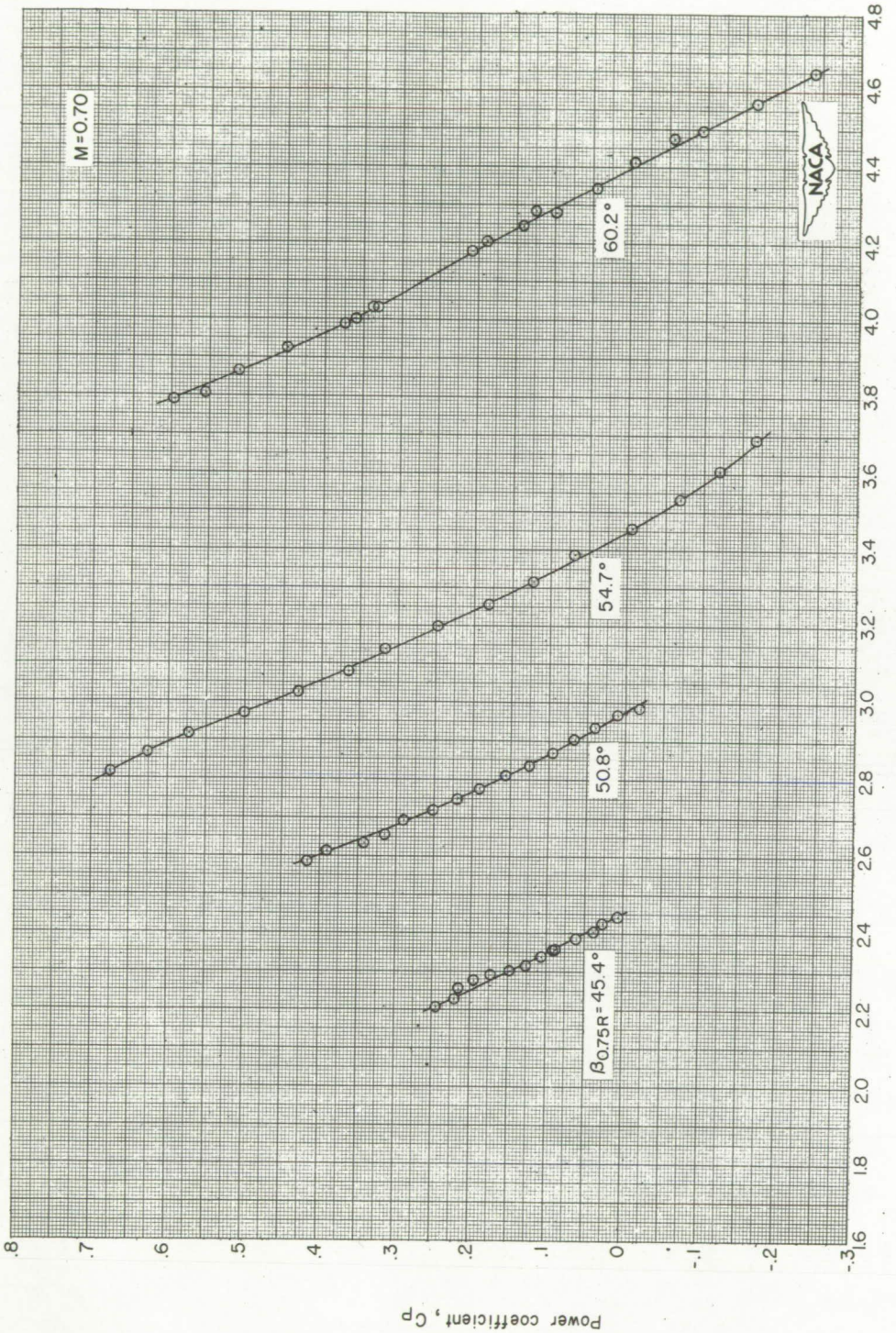

(b) Power coefficient.

Figure 8.- Continued.

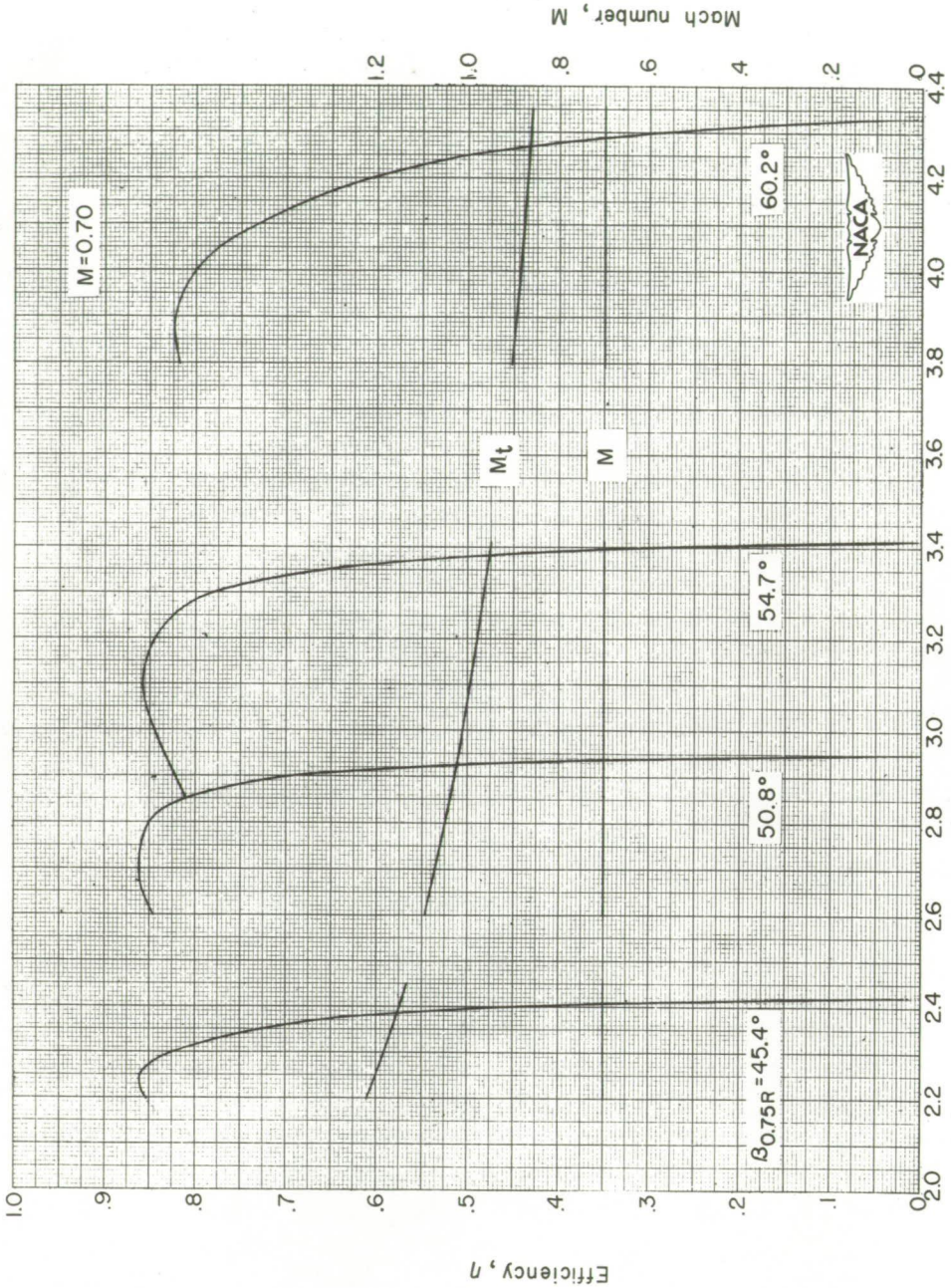

(c) Efficiency.

Figure 8.- Concluded.

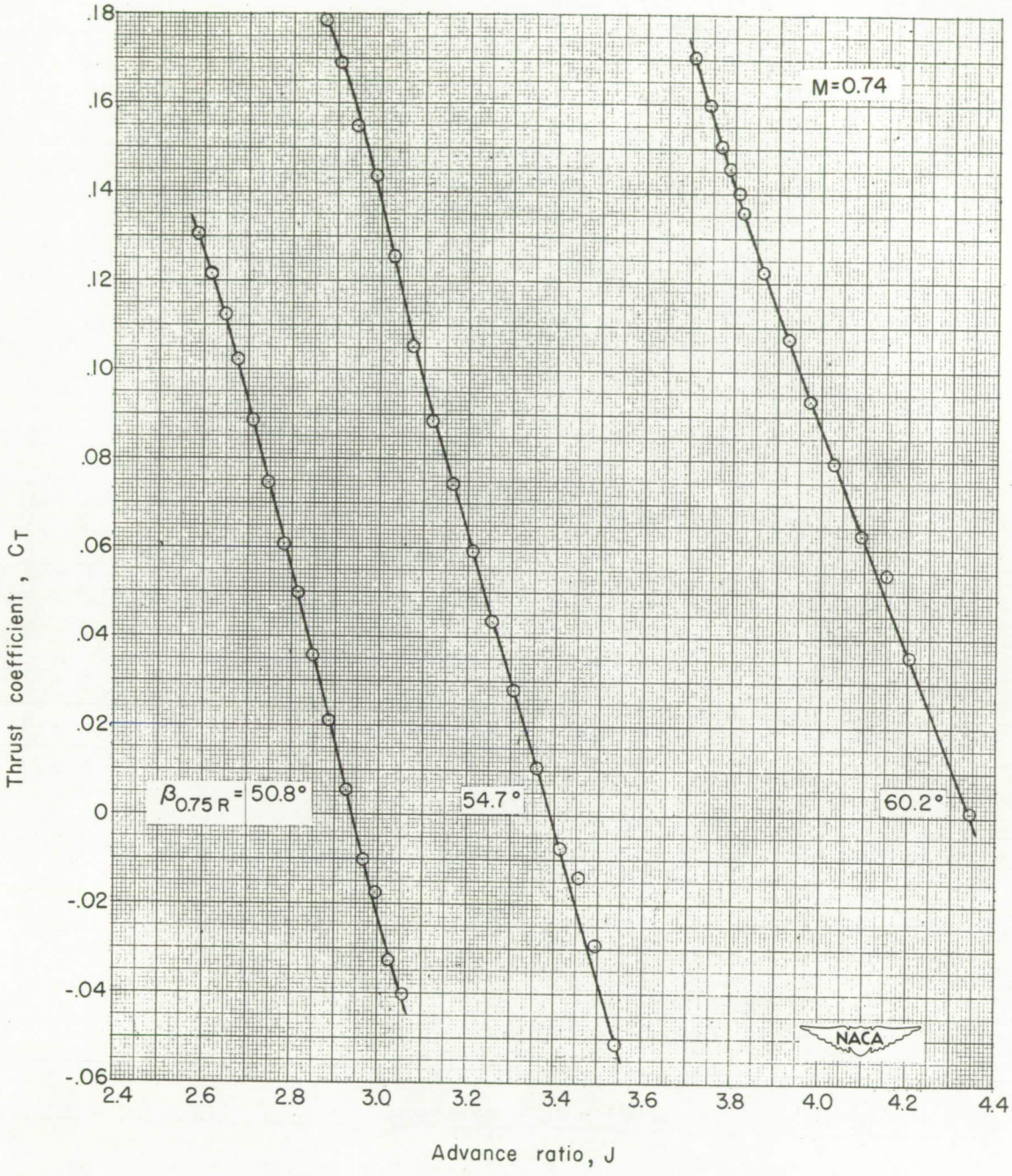

(a) Thrust coefficient.

Figure 9.- Characteristics of propeller. Forward Mach number 0.74.

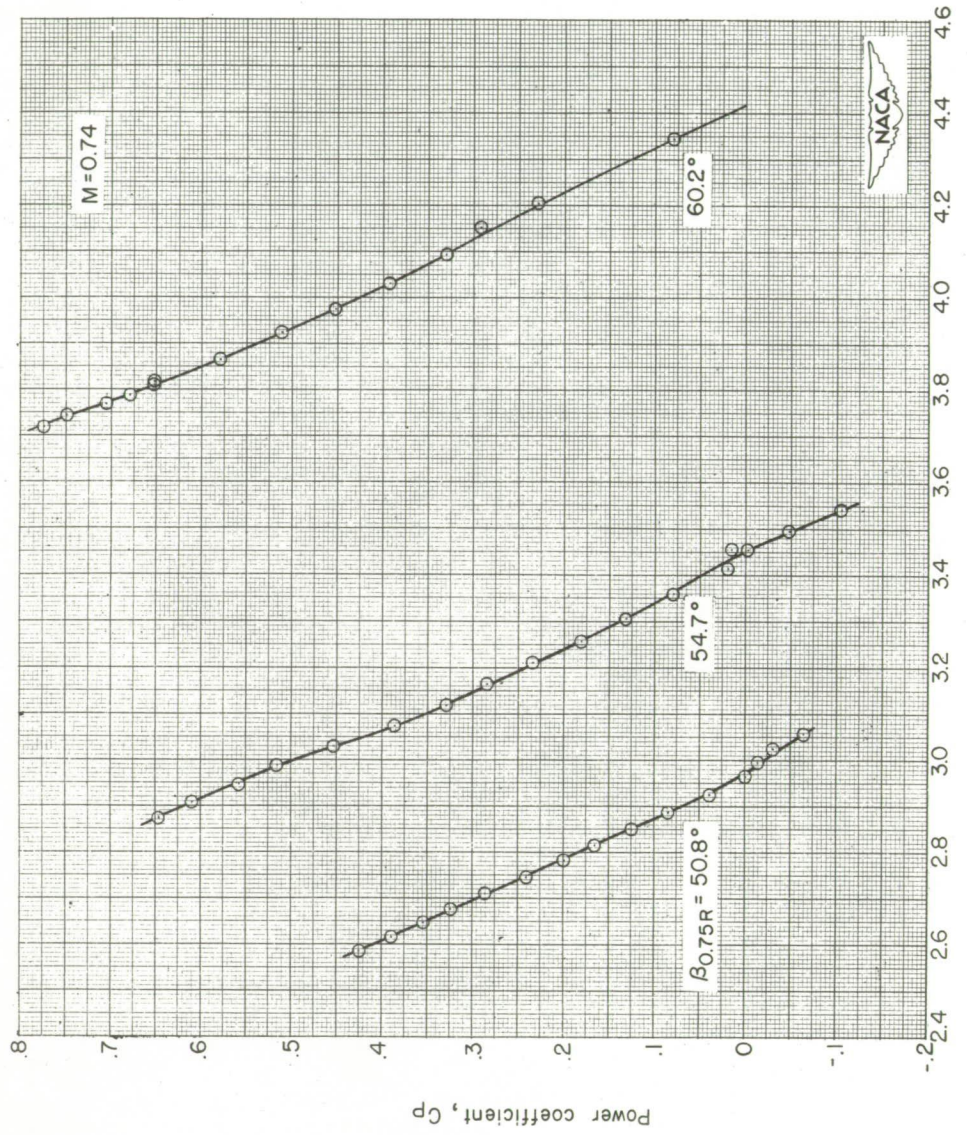

(b) Power coefficient.

Figure 9.- Continued.

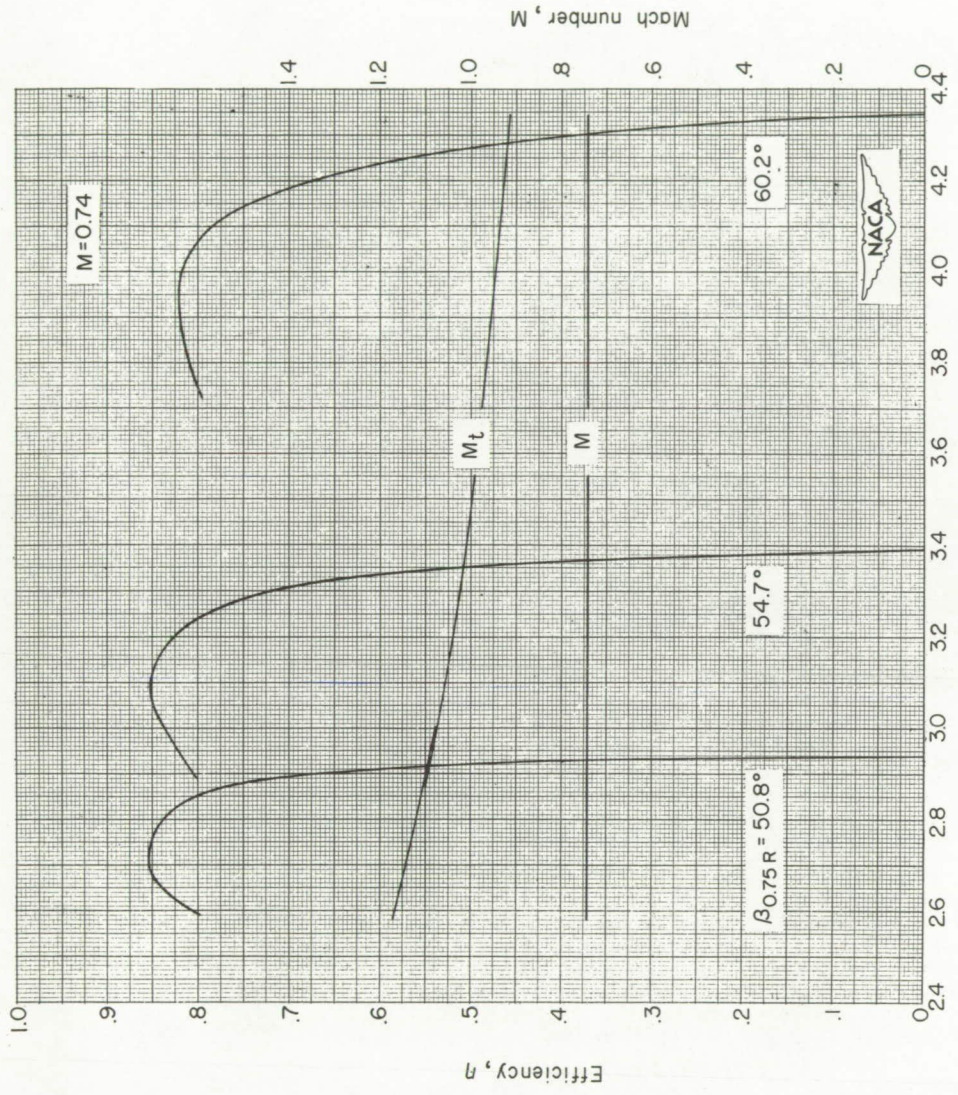

(c) Efficiency.

Figure 9.- Concluded.

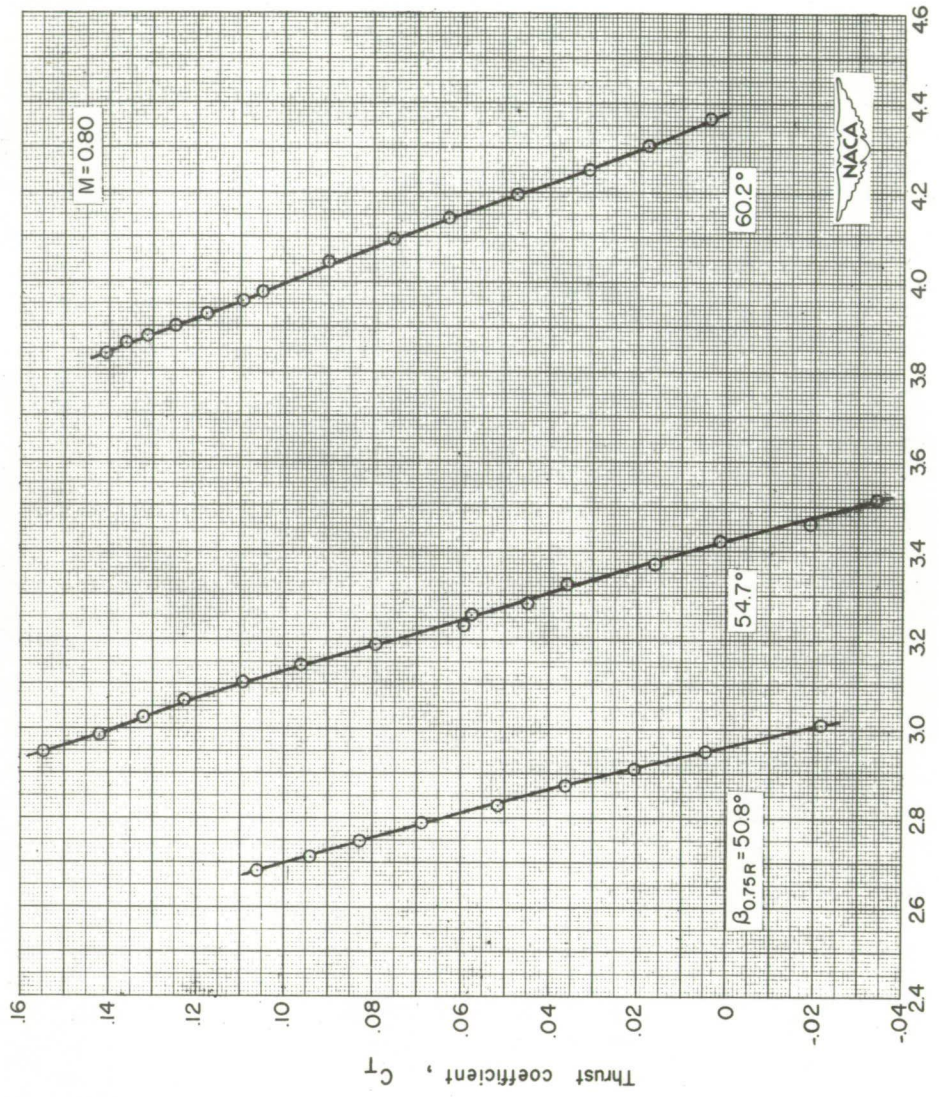

(a) Thrust coefficient.

Figure 10.- Characteristics of propeller. Forward Mach number 0.80.

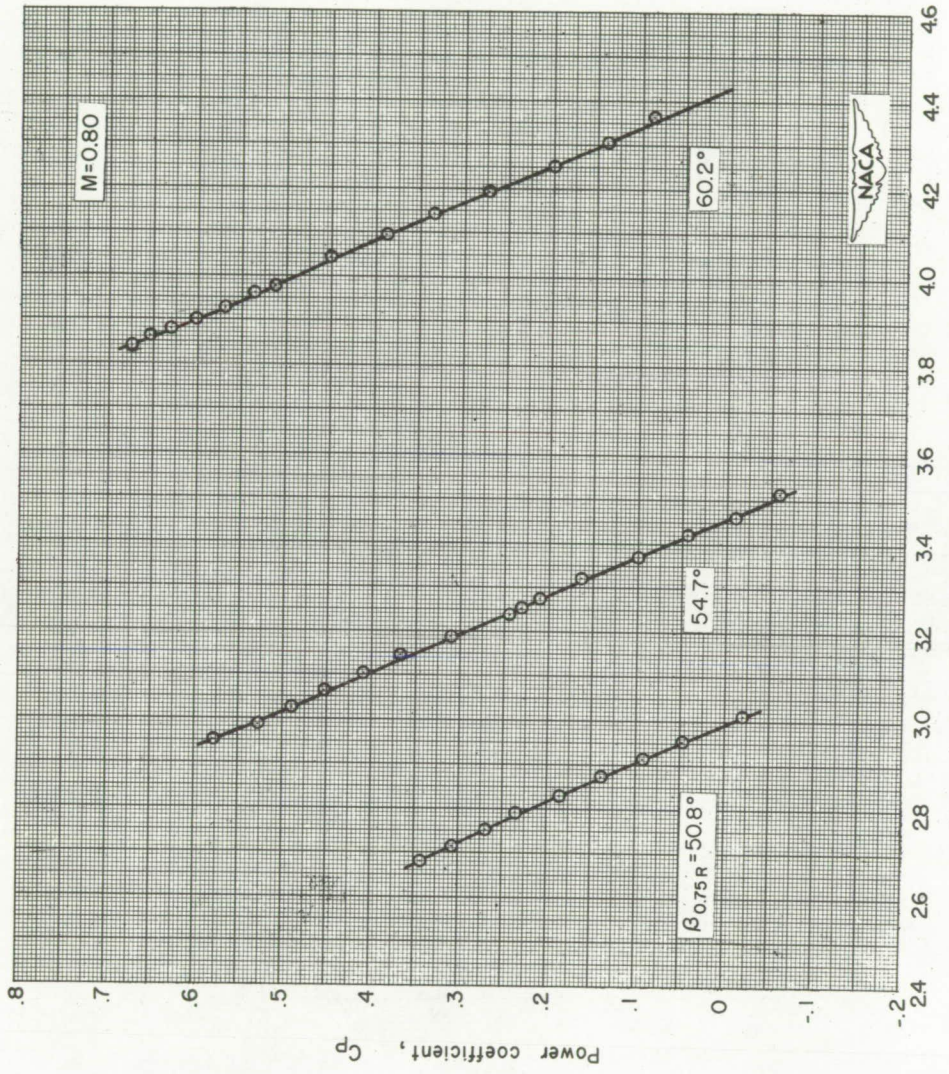

(b) Power coefficient.

Figure 10.- Continued.

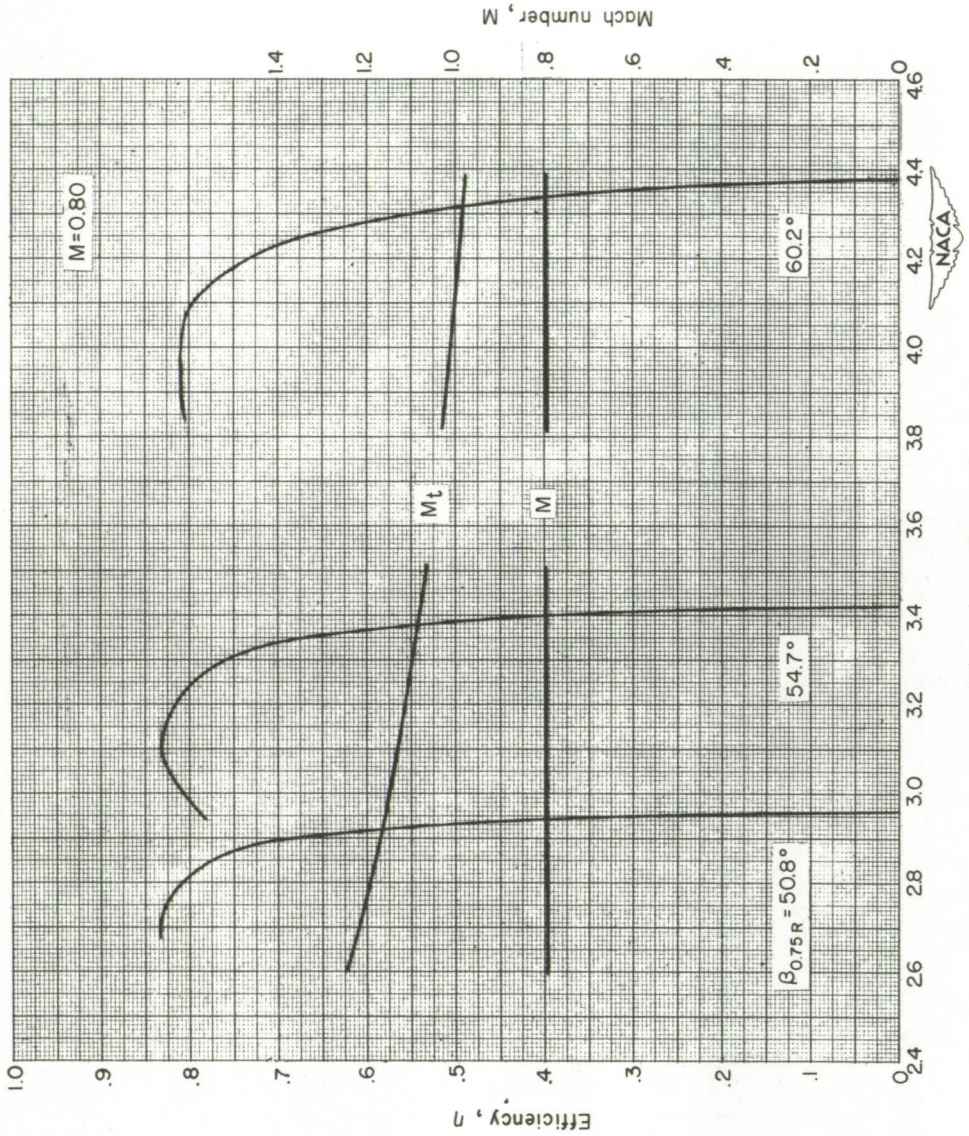

(c) Efficiency.

Figure 10.- Concluded.

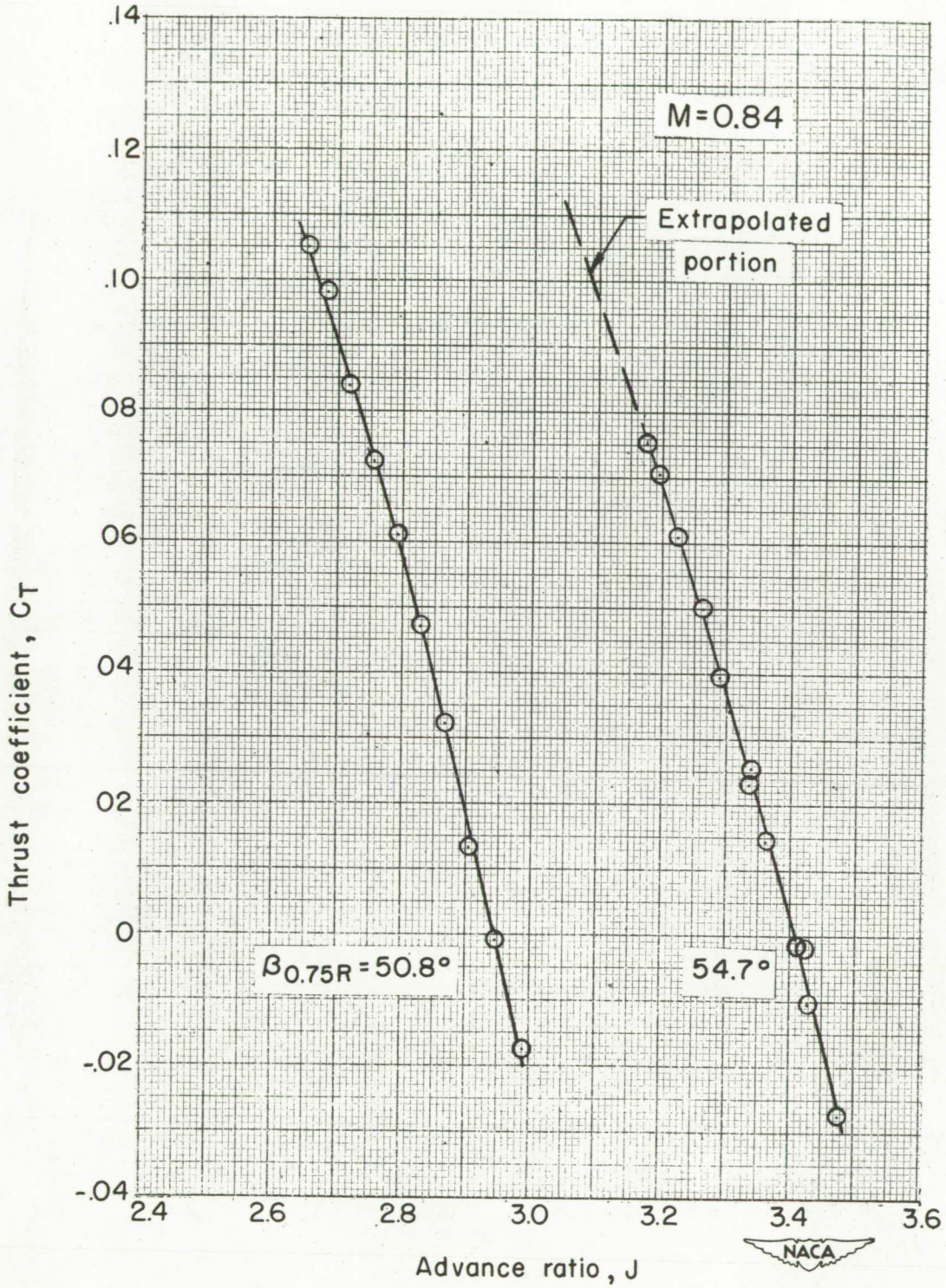

(a) Thrust coefficient.

Figure 11.- Characteristics of propeller. Forward Mach number 0.84.

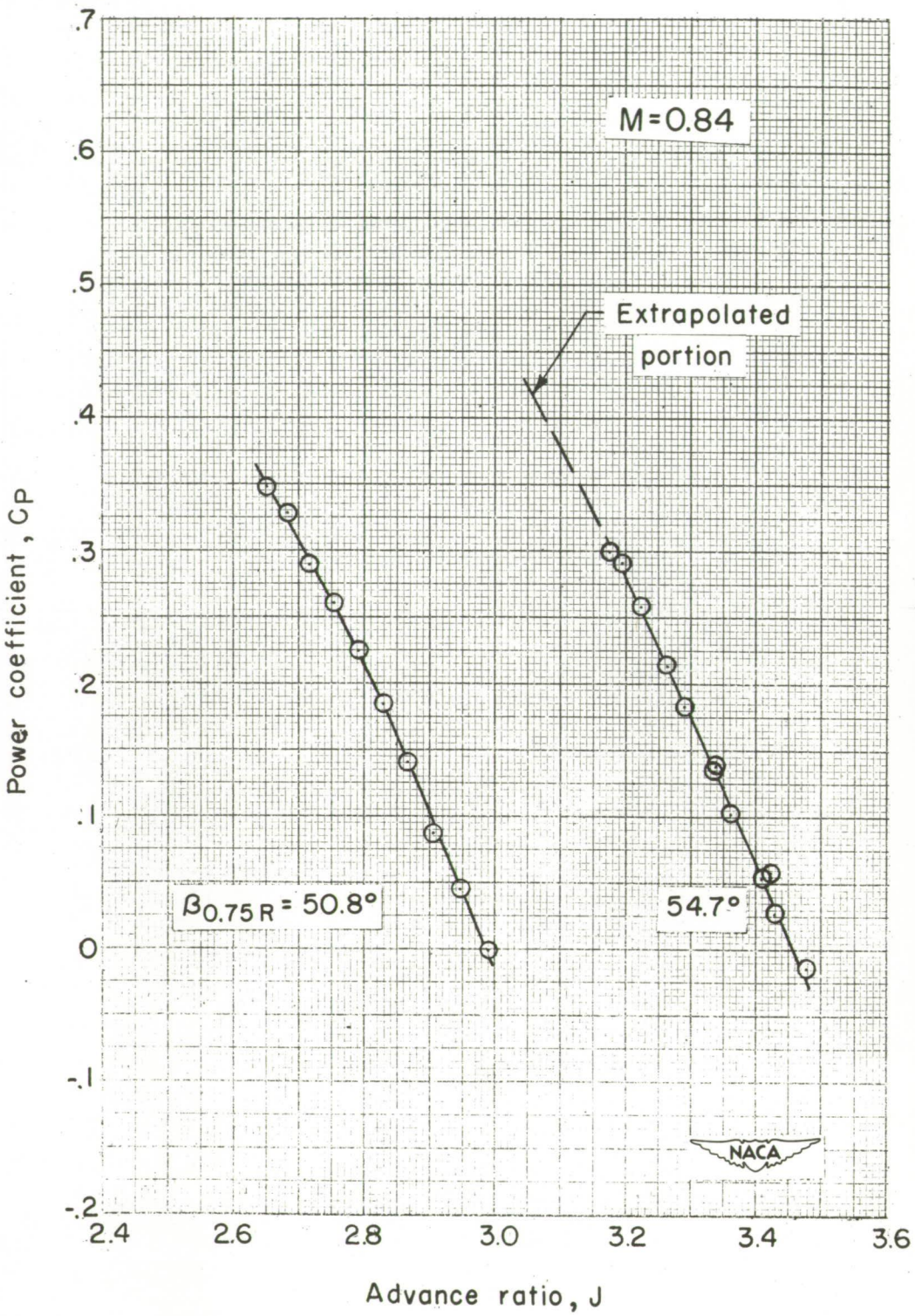

(b) Power coefficient.

Figure 11.- Continued.

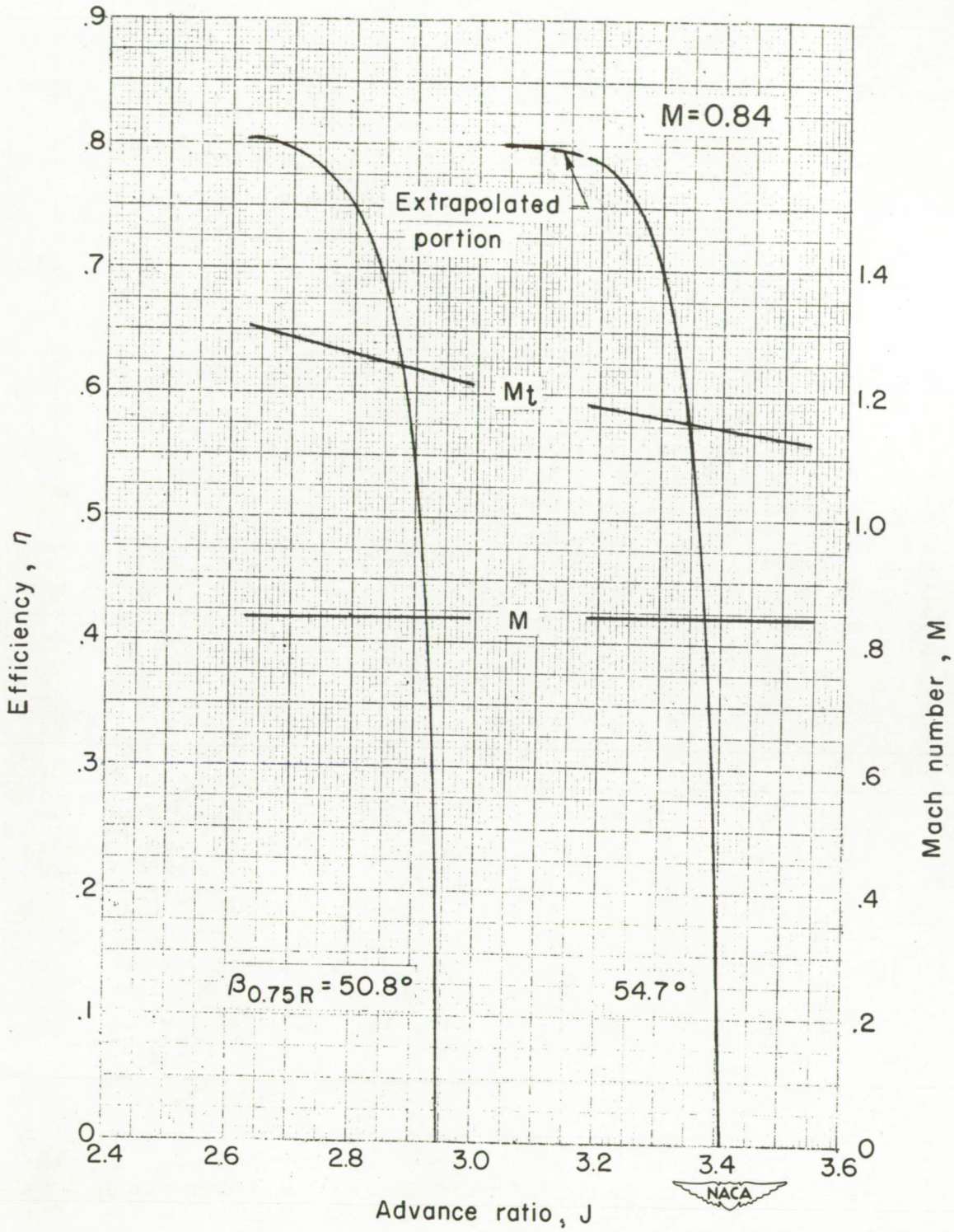

(c) Efficiency.

Figure 11.- Concluded.

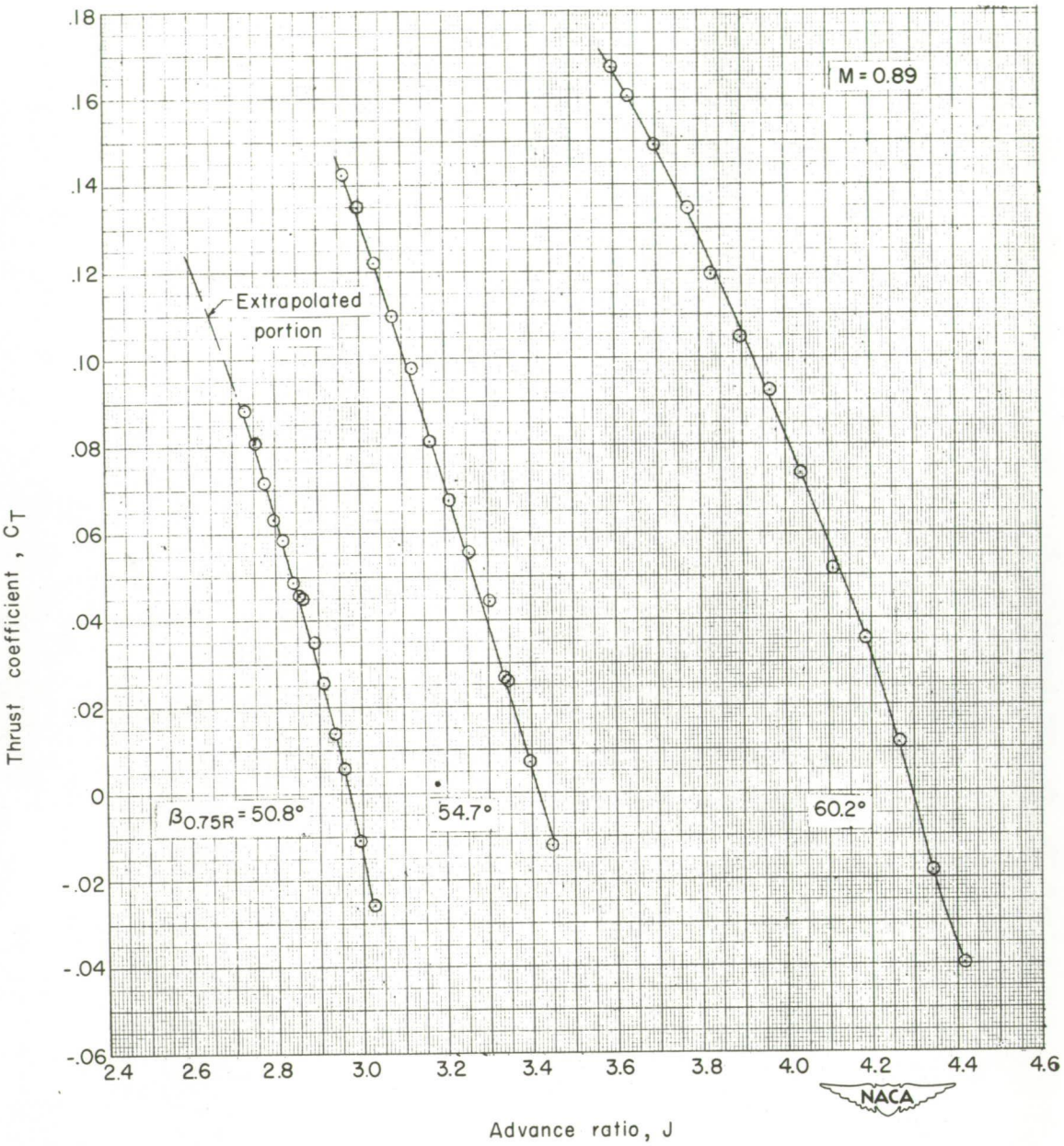

(a) Thrust coefficient.

Figure 12.- Characteristics of propeller. Forward Mach number 0.89.

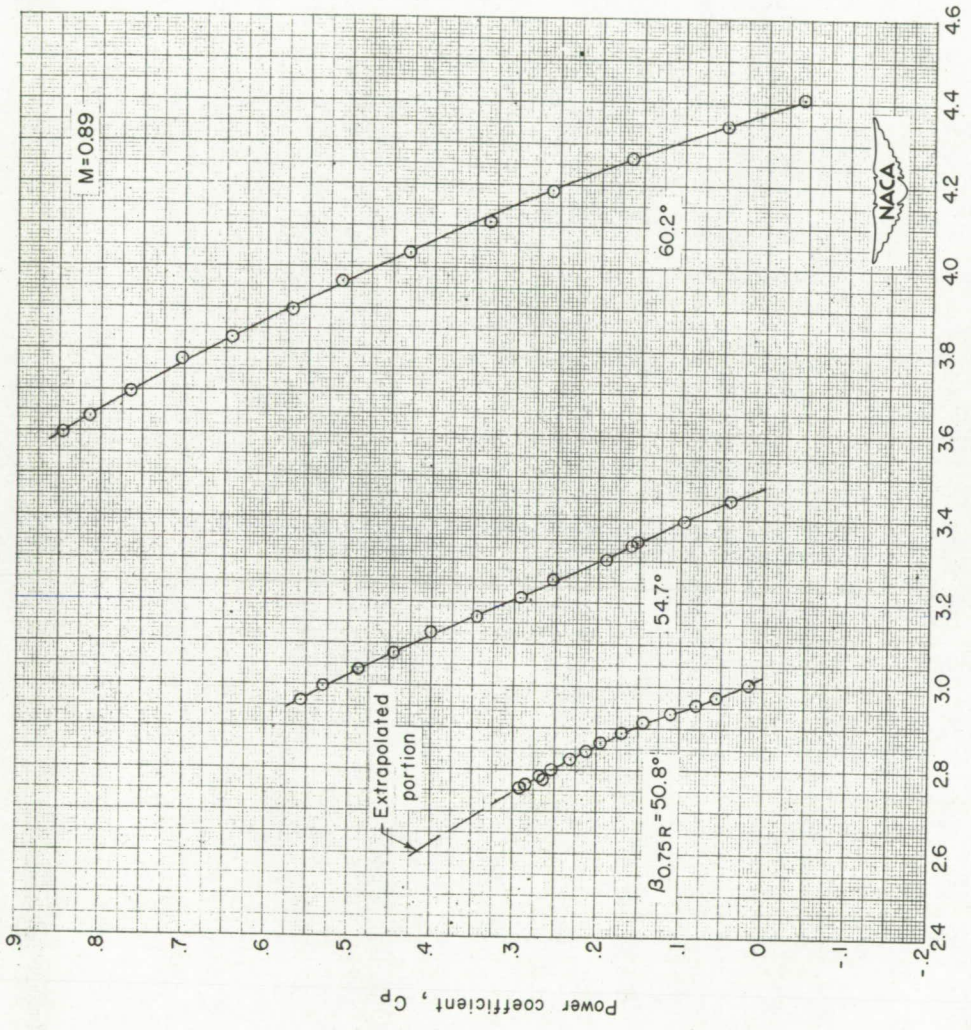

(b) Power coefficient.

Figure 12.- Continued.

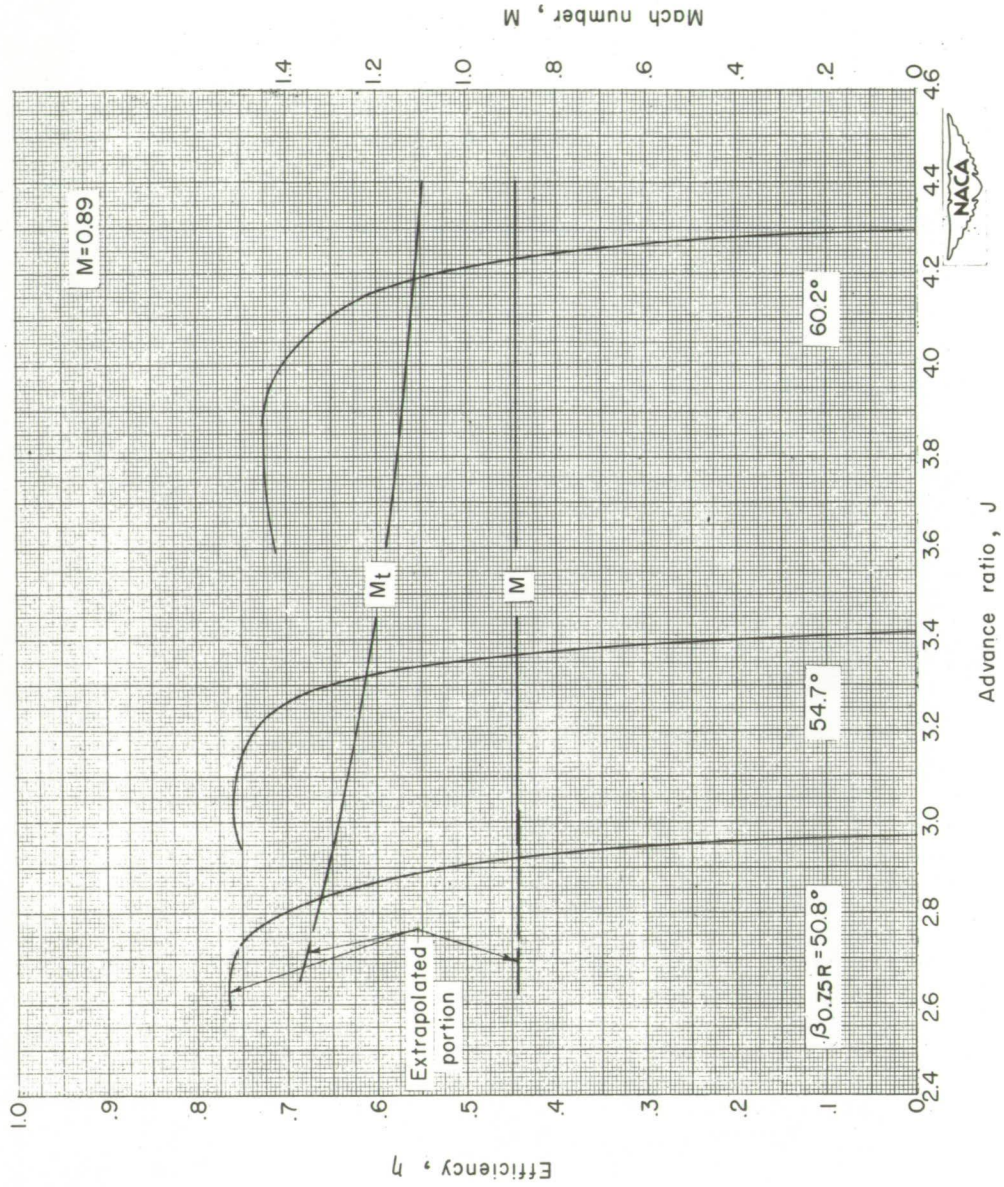

(c) Efficiency.

Figure 12.- Concluded.

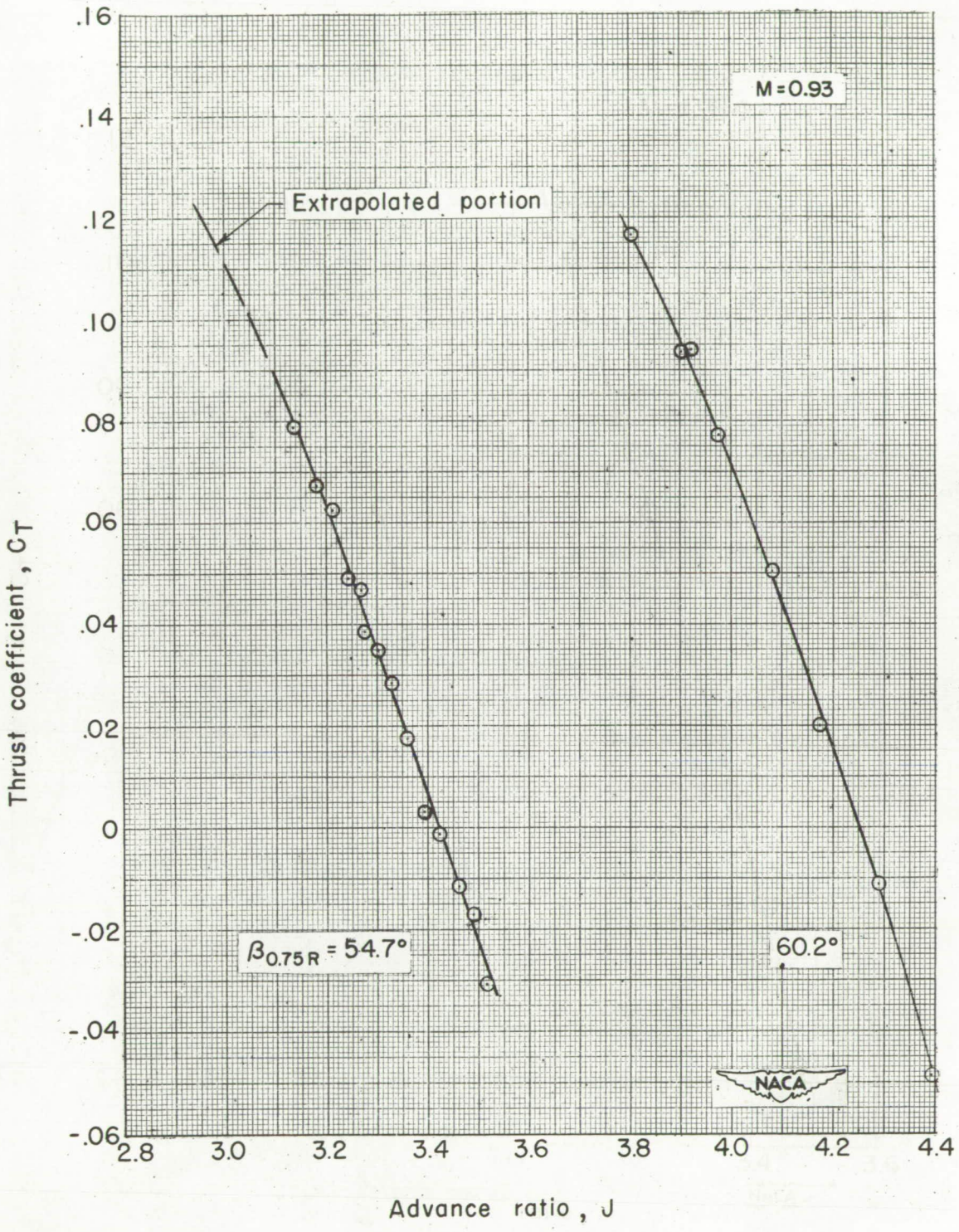

(a) Thrust coefficient.

Figure 13.- Characteristics of propeller. Forward Mach number 0.93.

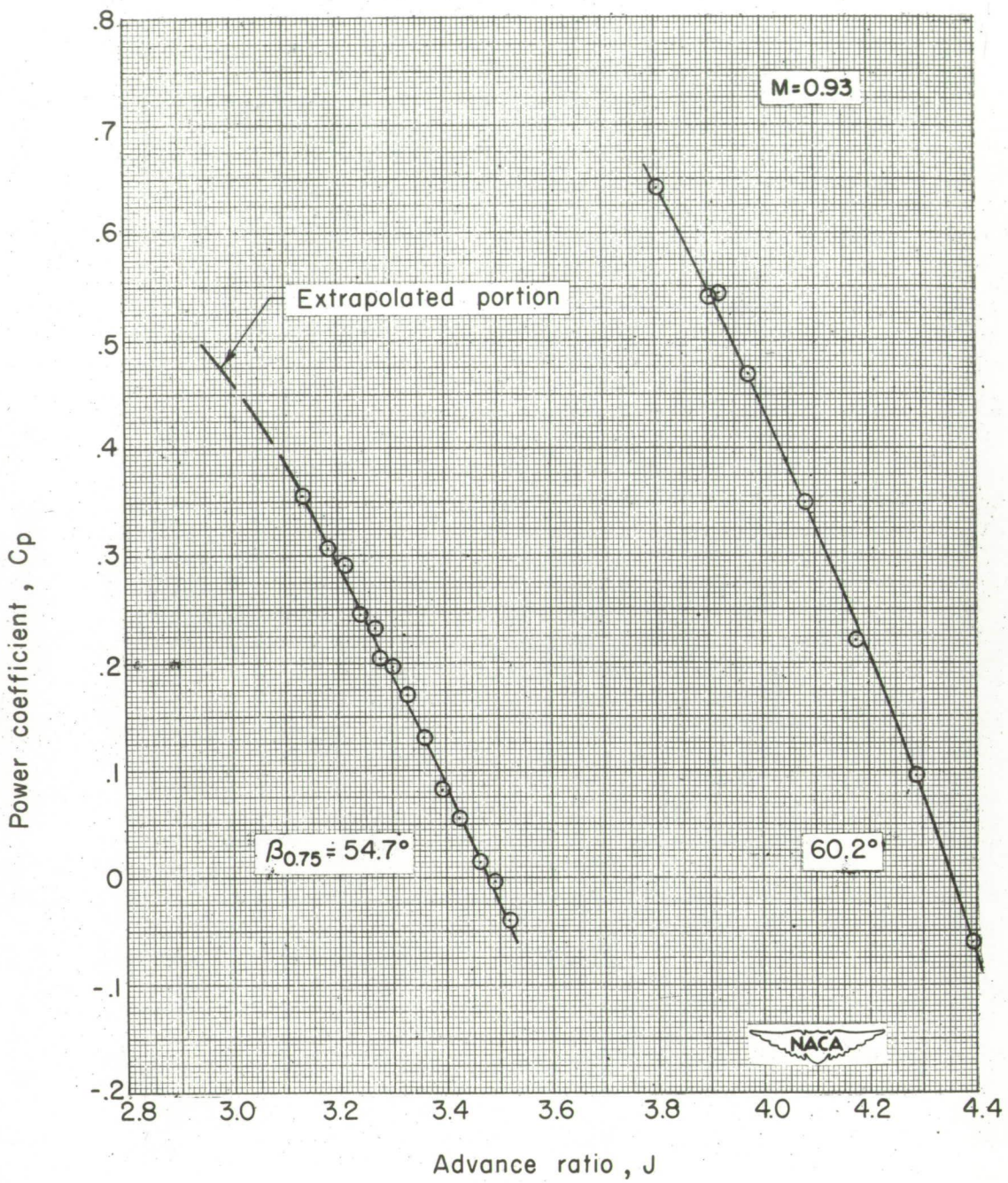

(b) Power coefficient.

Figure 13.- Continued.

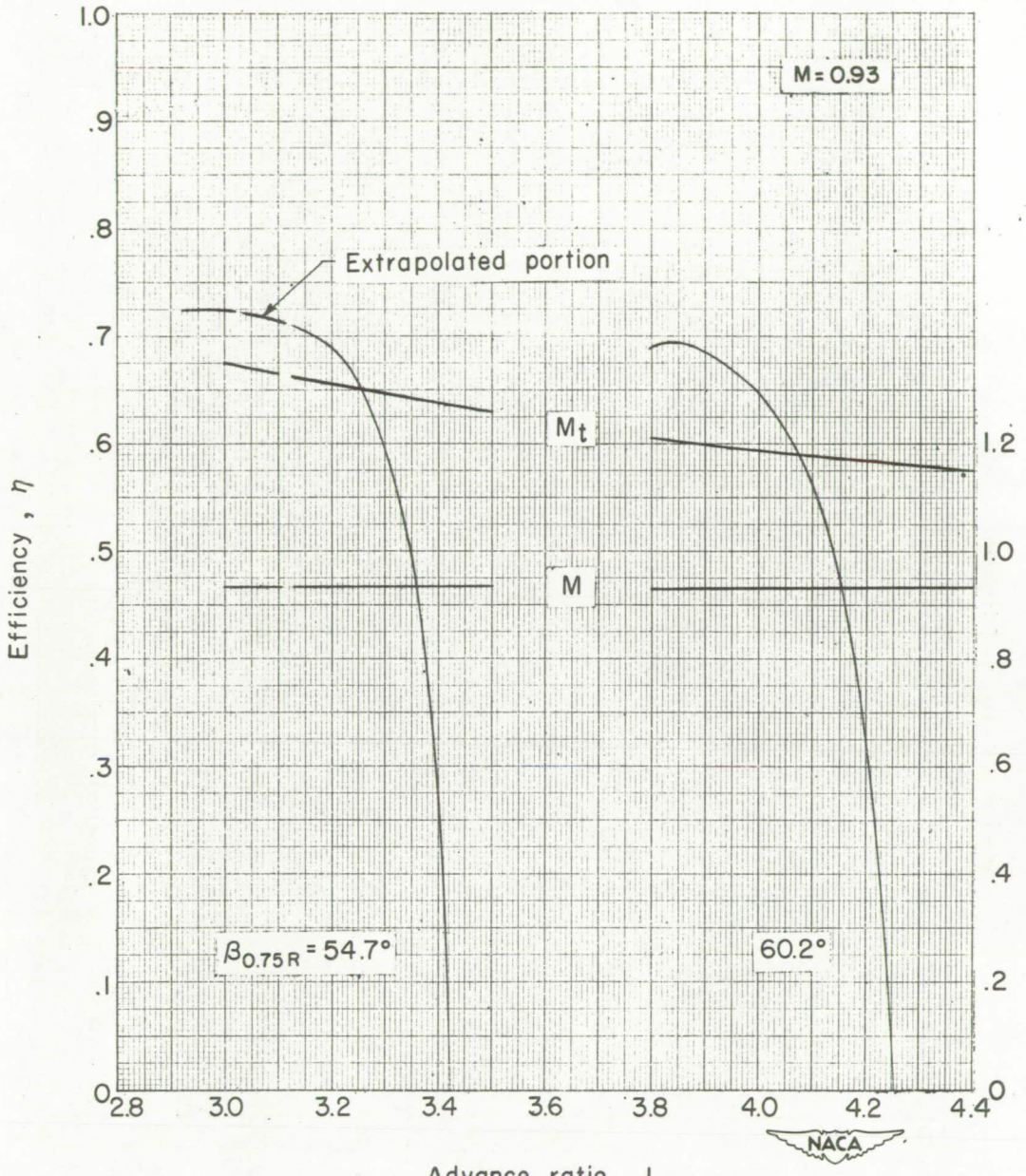

(c) Efficiency.

Figure 13.- Concluded.

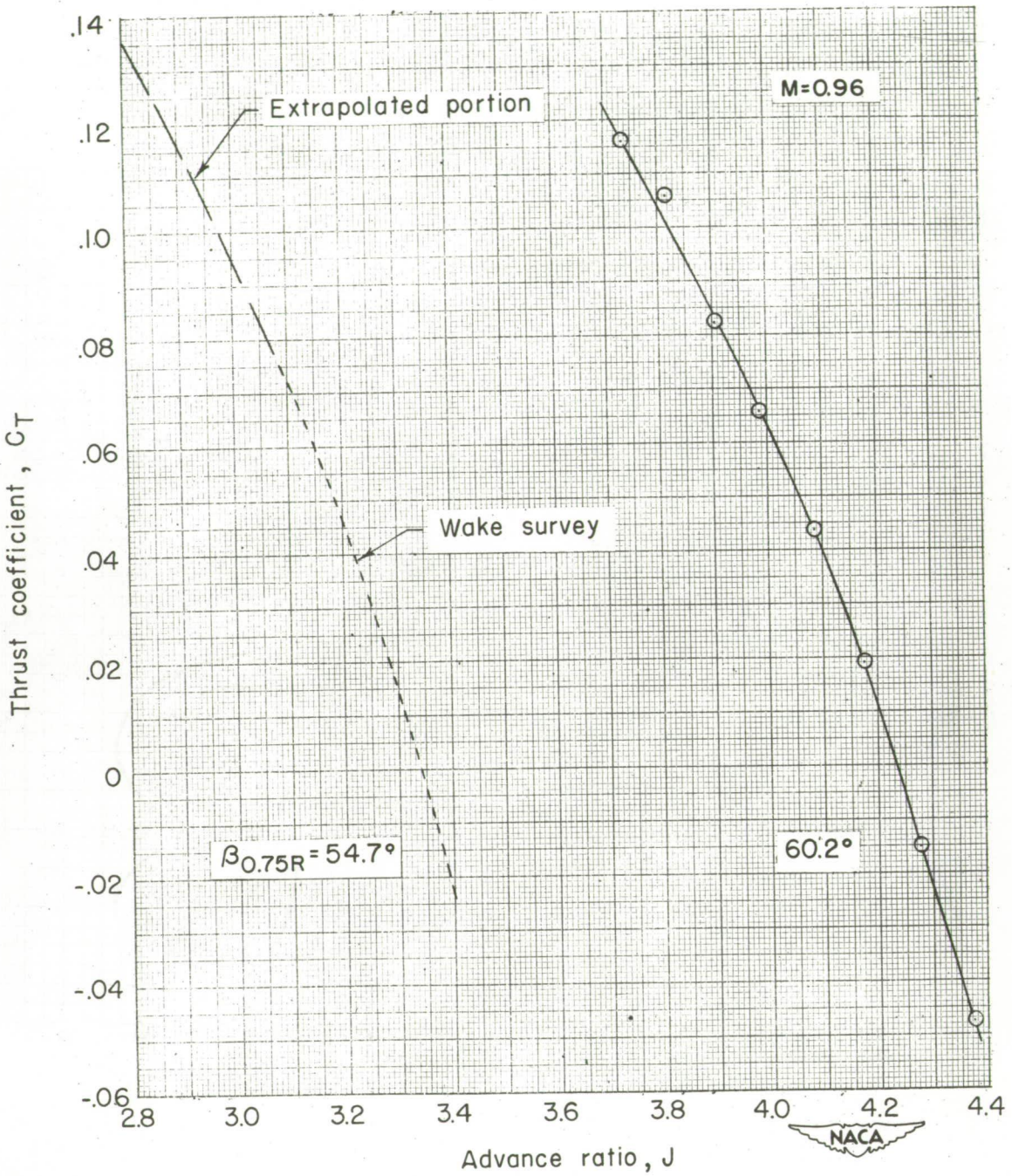

(a) Thrust coefficient.

Figure 14.- Characteristics of propeller. Forward Mach number 0.96.

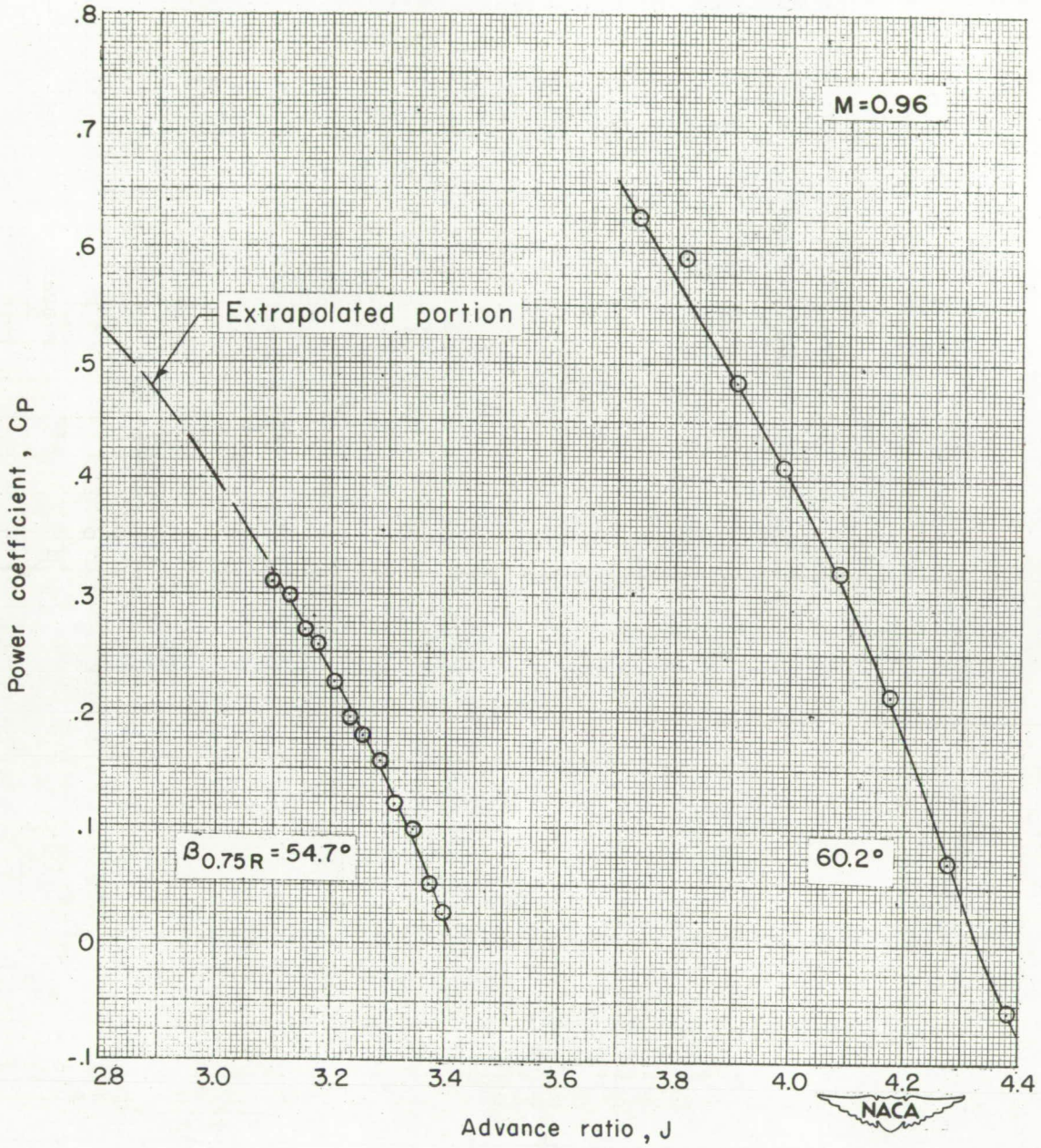

(b) Power coefficient.

Figure 14.- Continued.

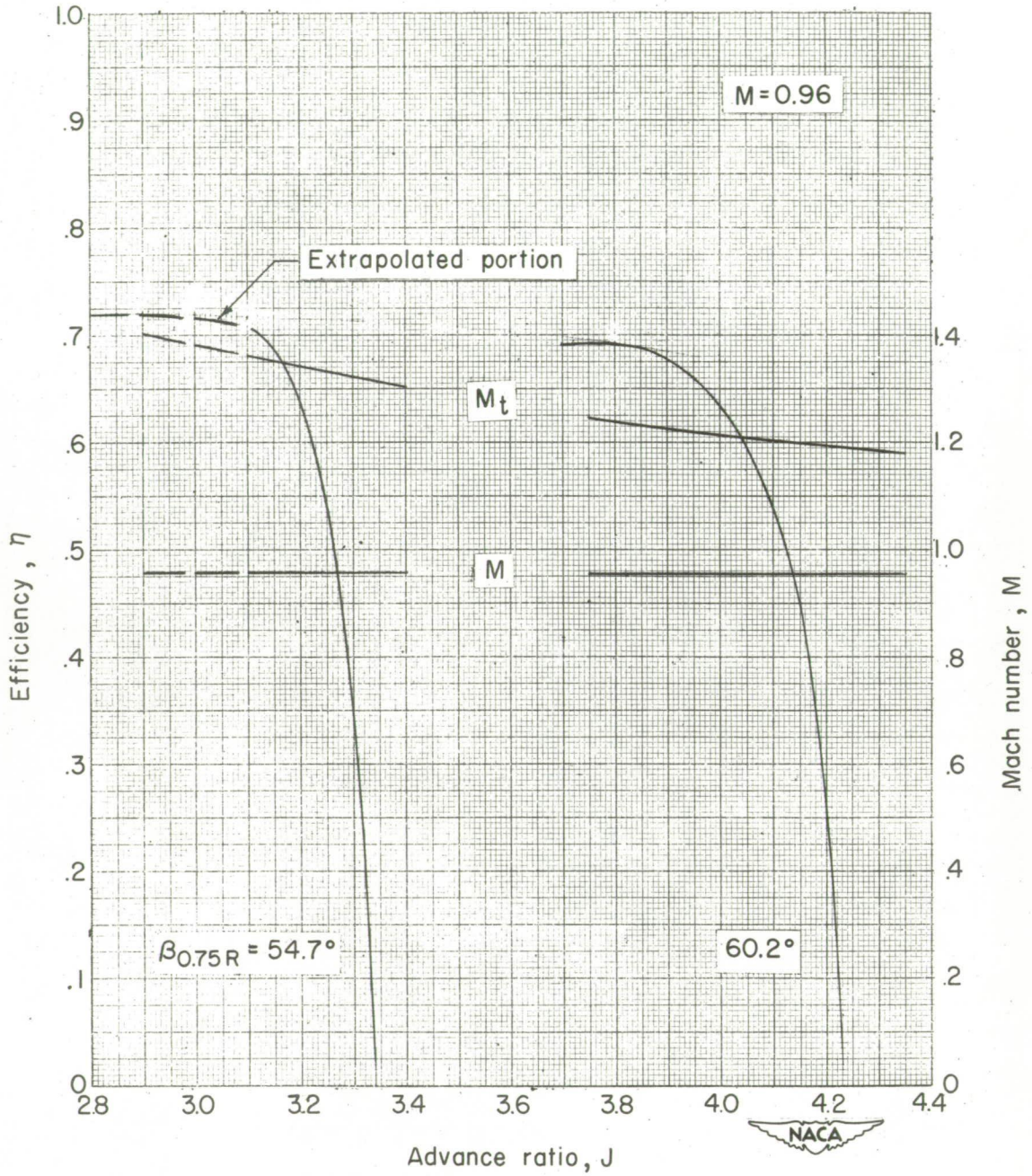

(c) Efficiency.

Figure 14.- Concluded.

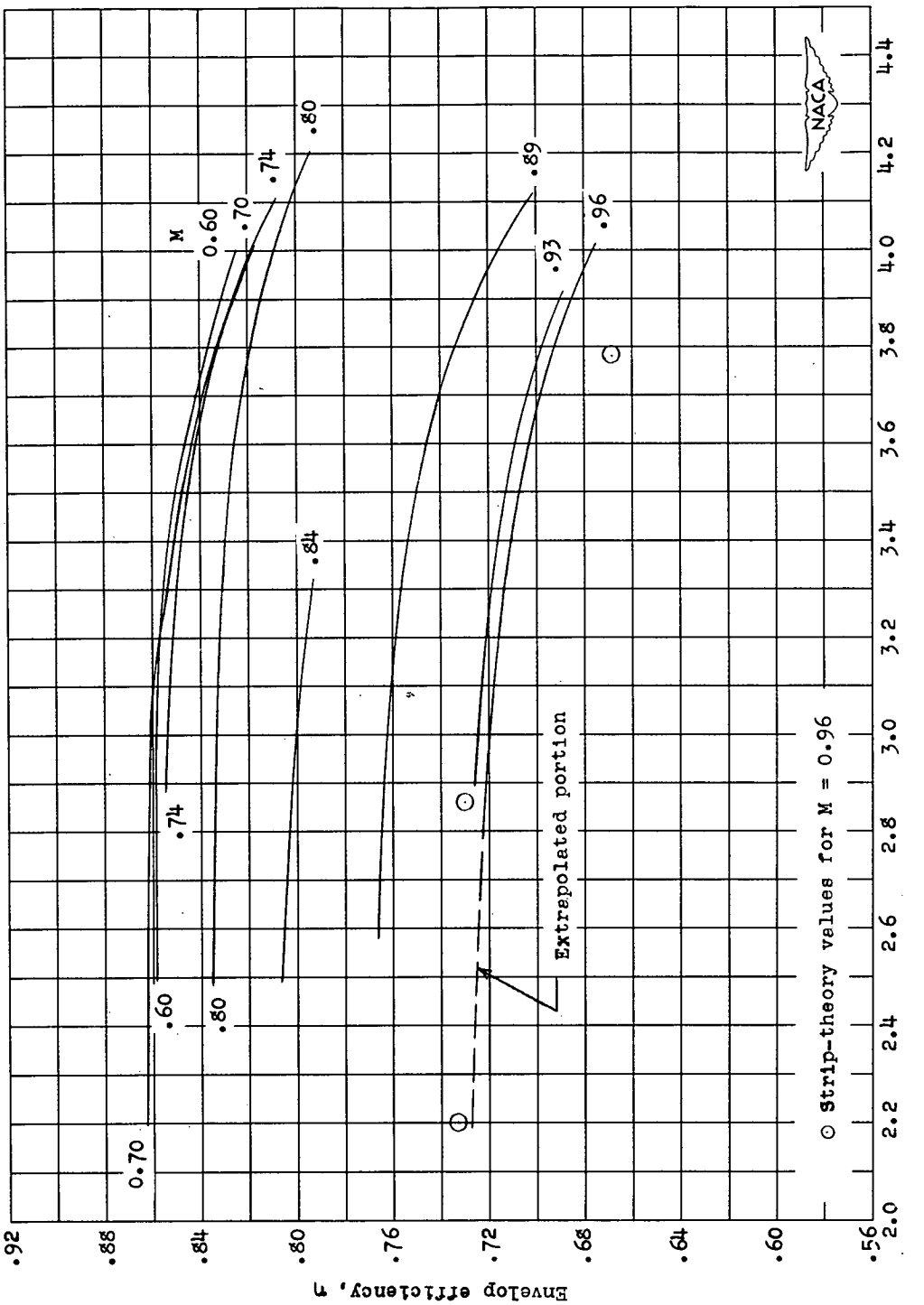

Figure 15.- Variation of envelop efficiency with advance ratio for various forward Mach numbers.

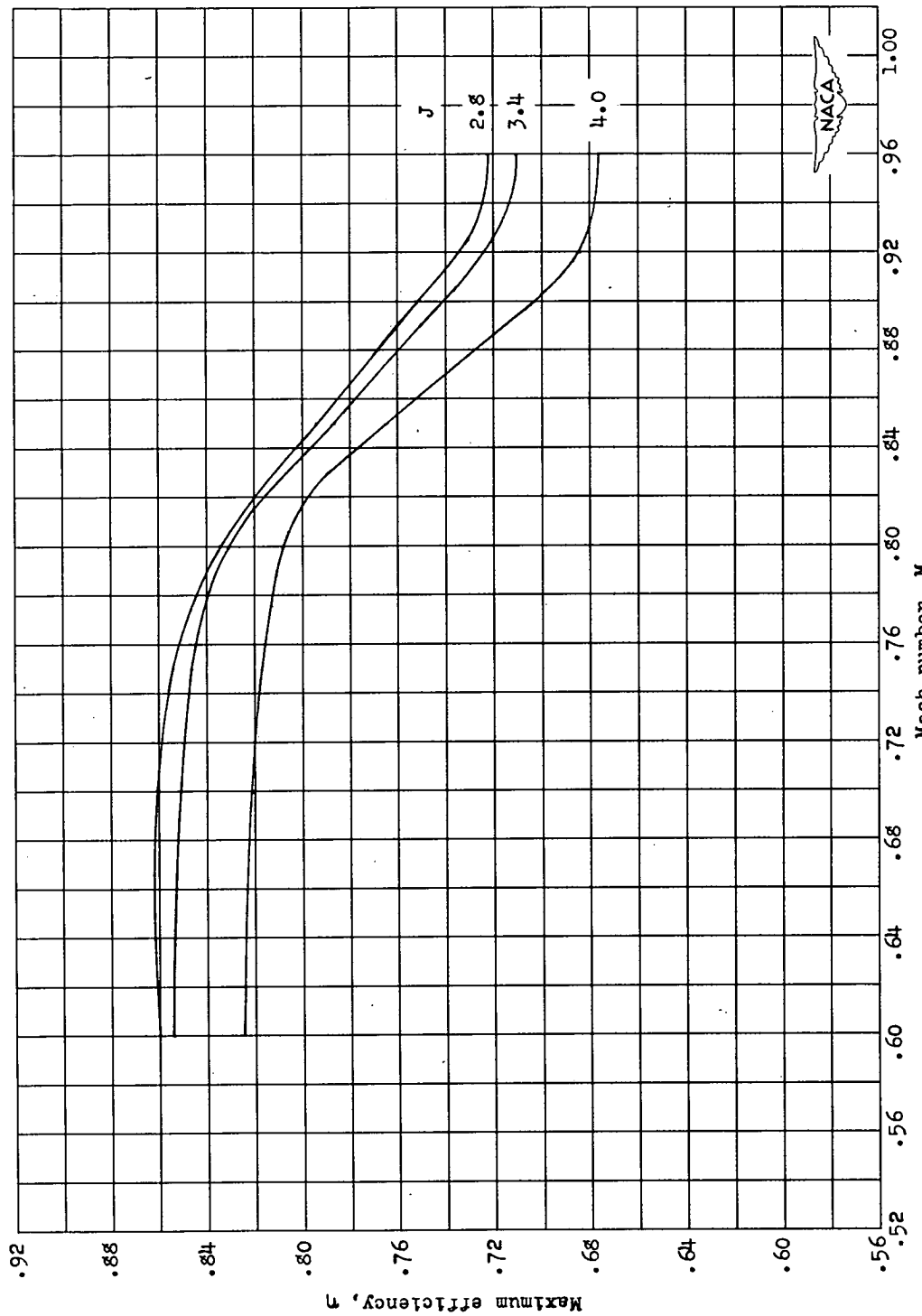

Figure 16.- Variation of maximum propeller efficiency with forward Mach number for several values of advance ratio.

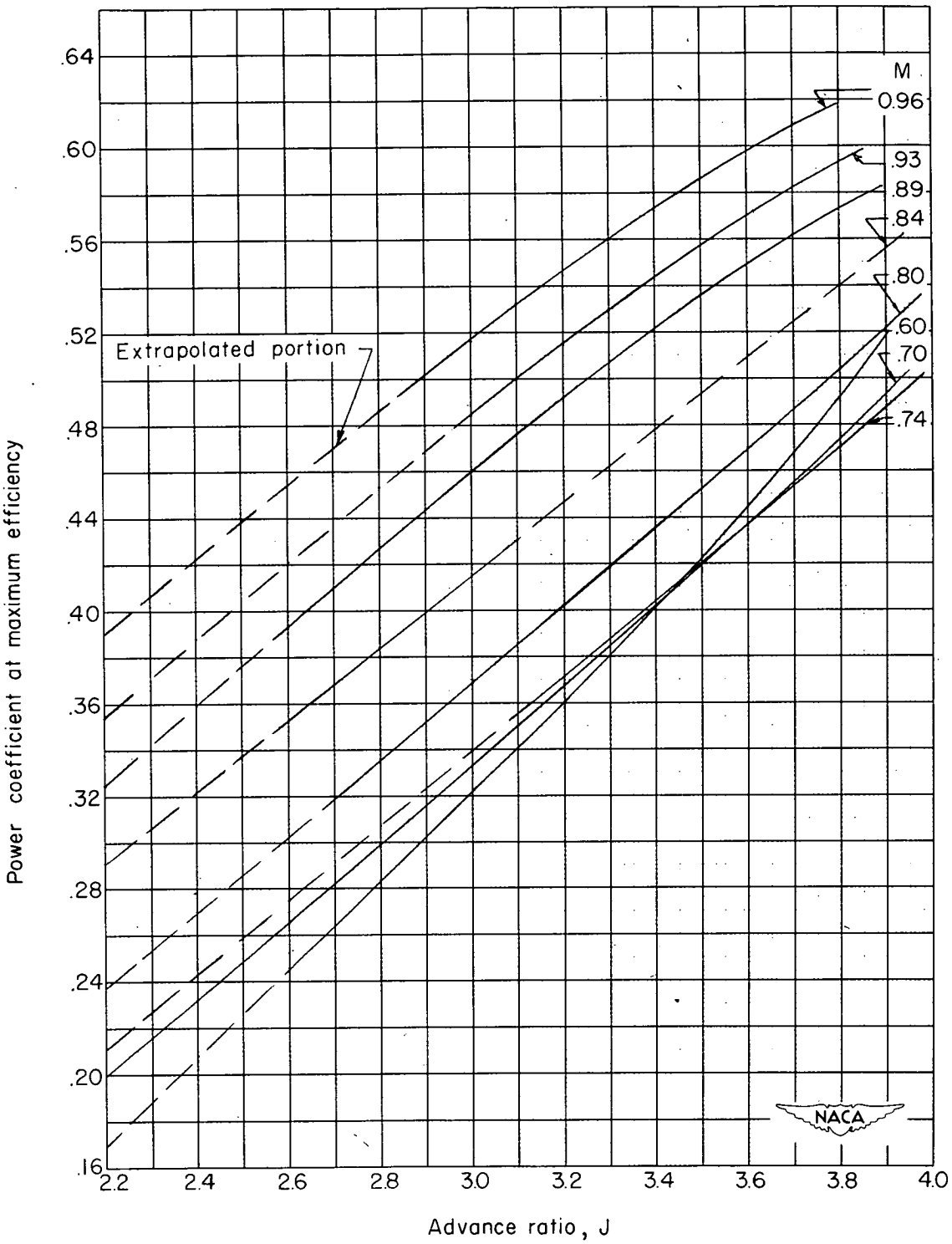

Figure 17.- Variation of power coefficient at maximum efficiency with advance ratio.

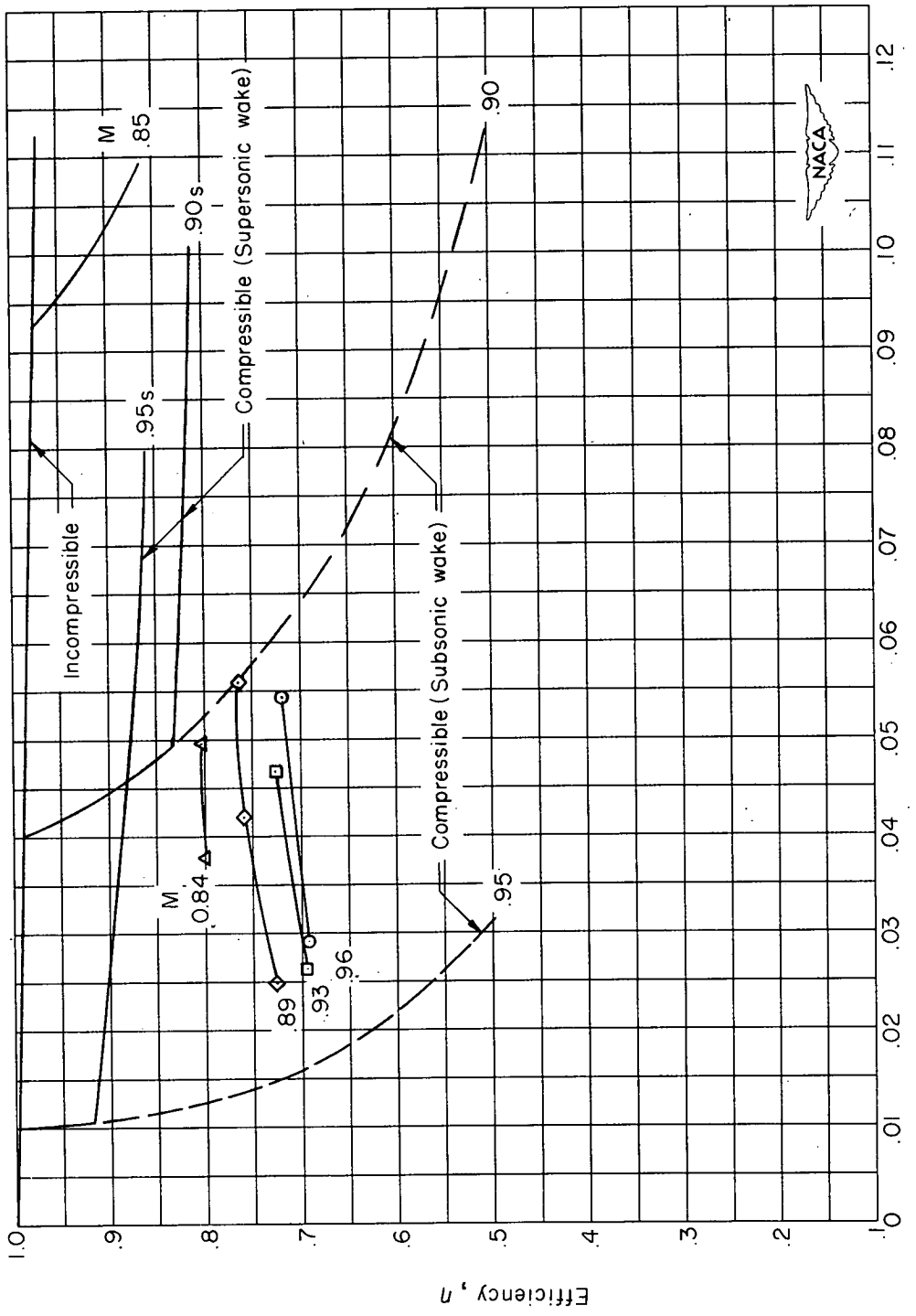

Figure 18.- Variation of maximum efficiency with power loading for several forward Mach numbers, (fig. 13 of ref. 8).

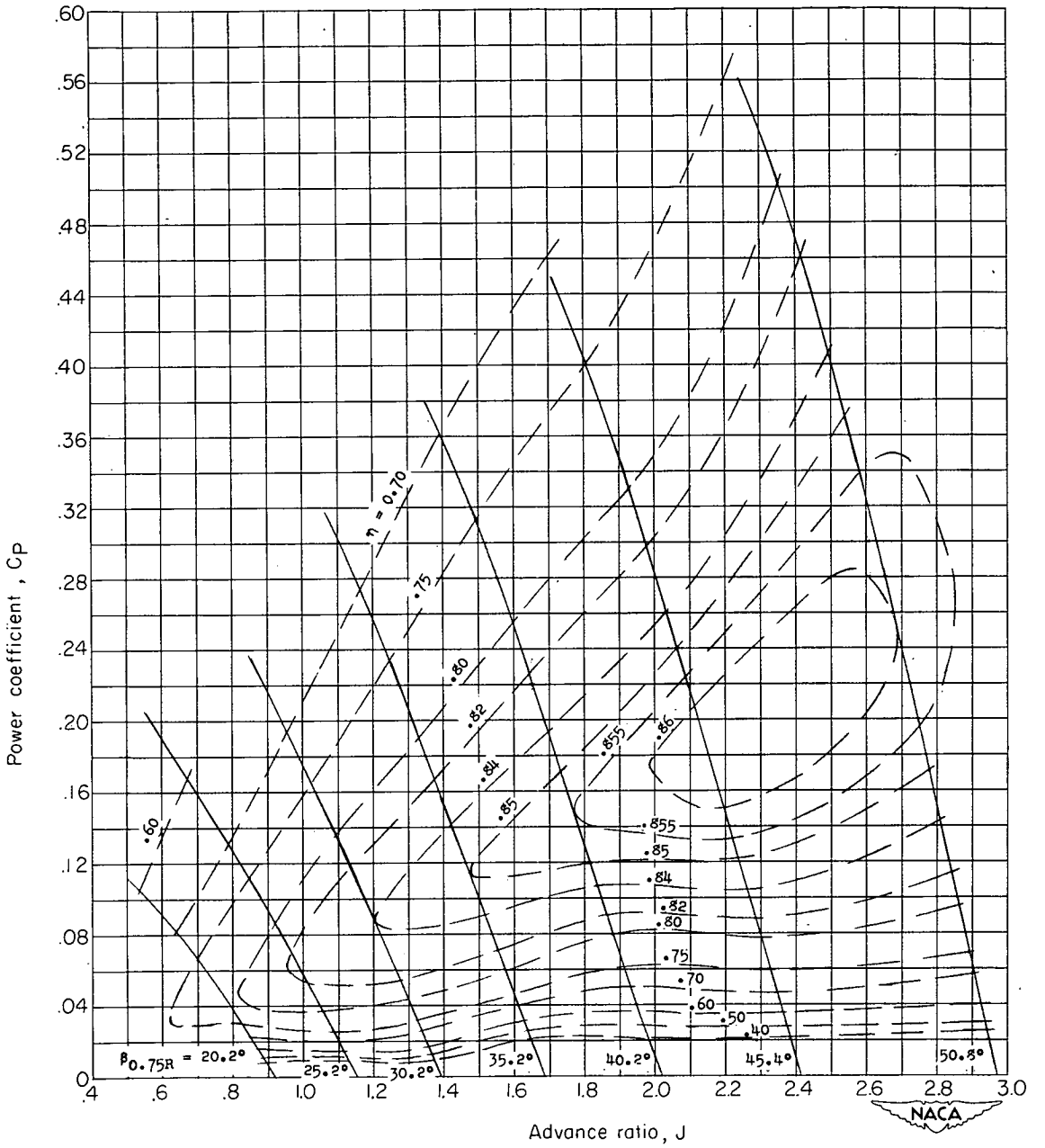

(a) 1600 rpm; M < 0.67.

Figure 19.- Operating charts for propeller. B = 3.

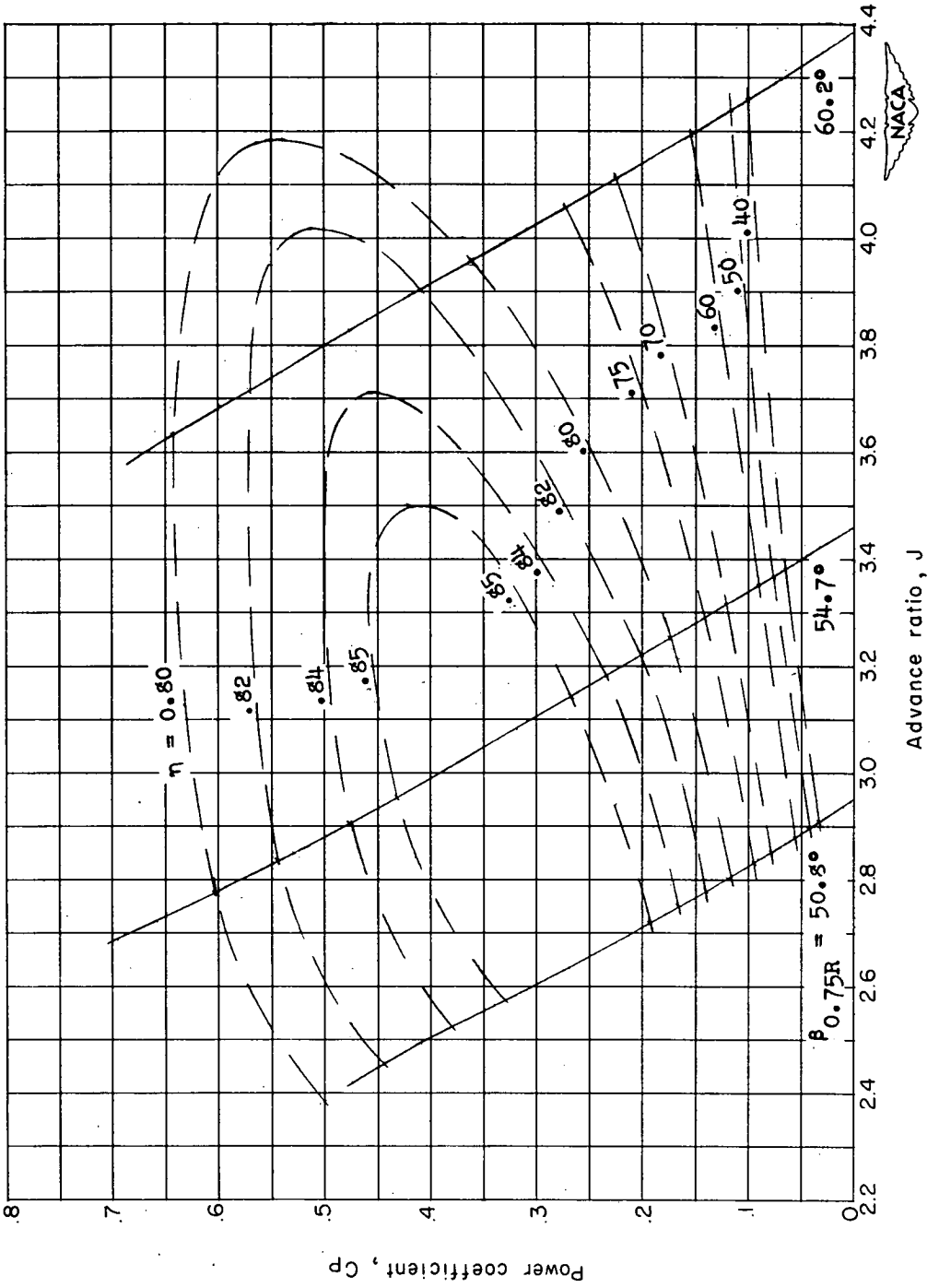

(b) M = 0.60.

Figure 19.- Continued.

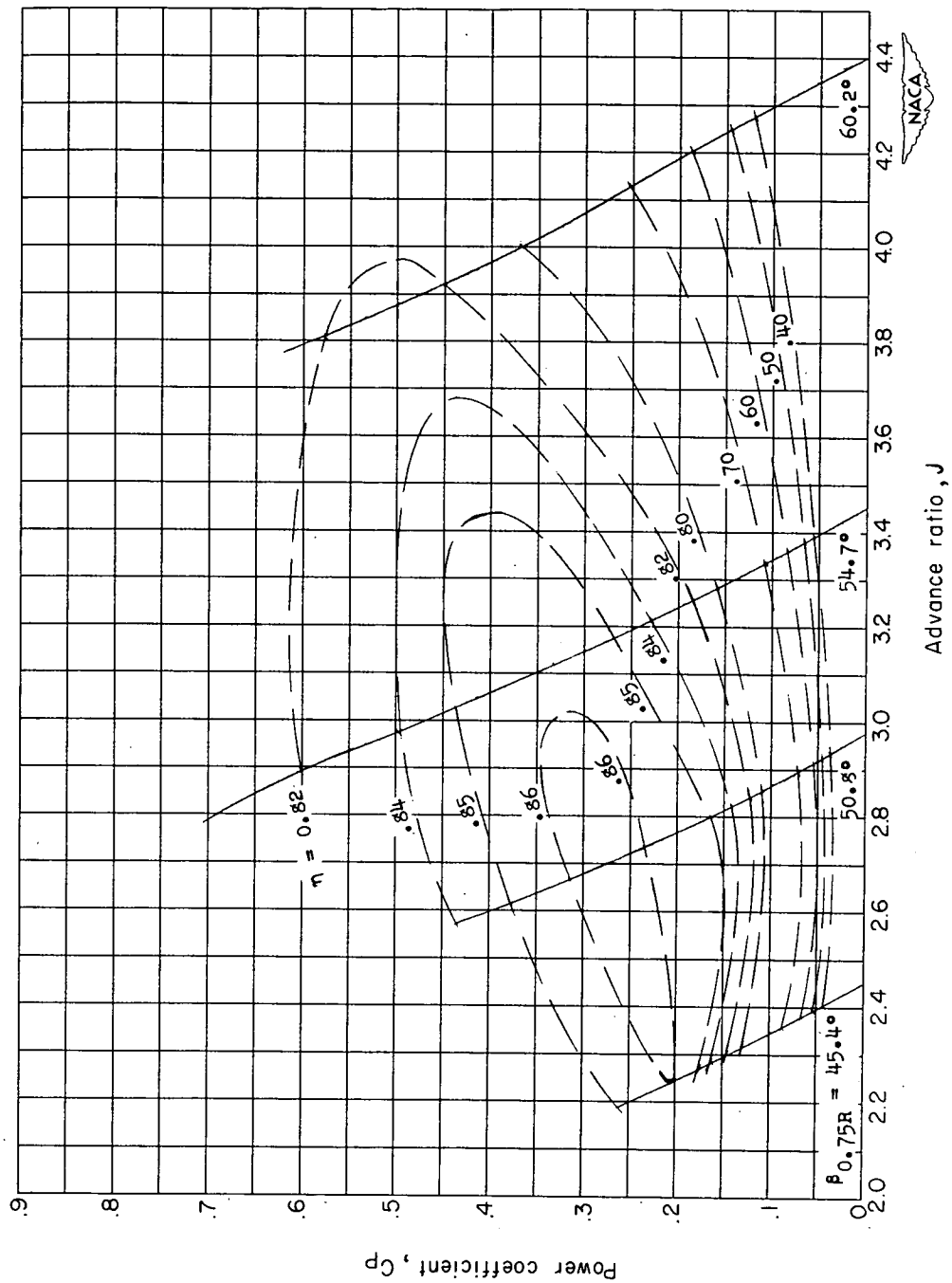

(c) M = 0.70.

Figure 19.- Continued.

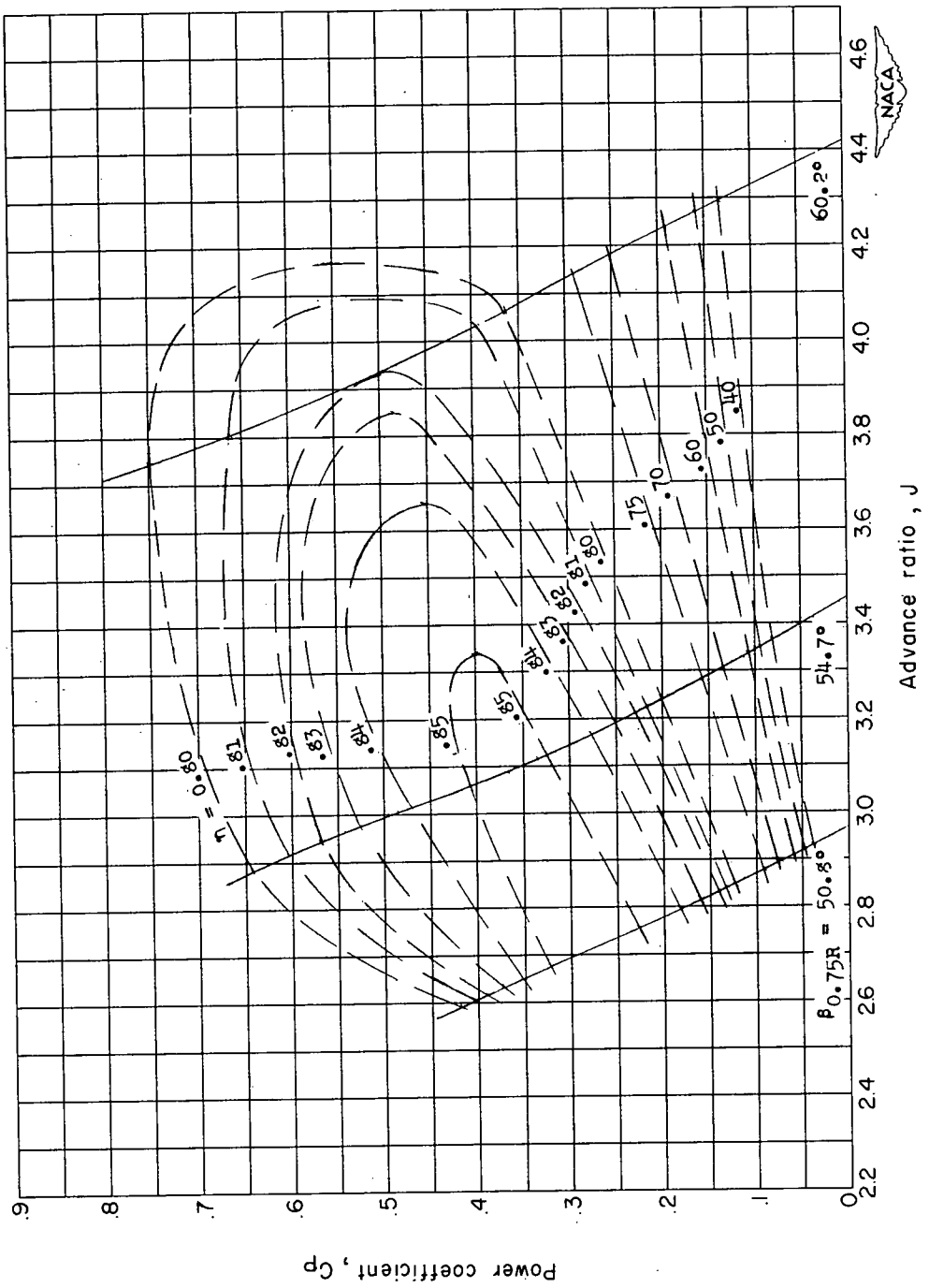

(d) M = 0.74.

Figure 19.- Continued.

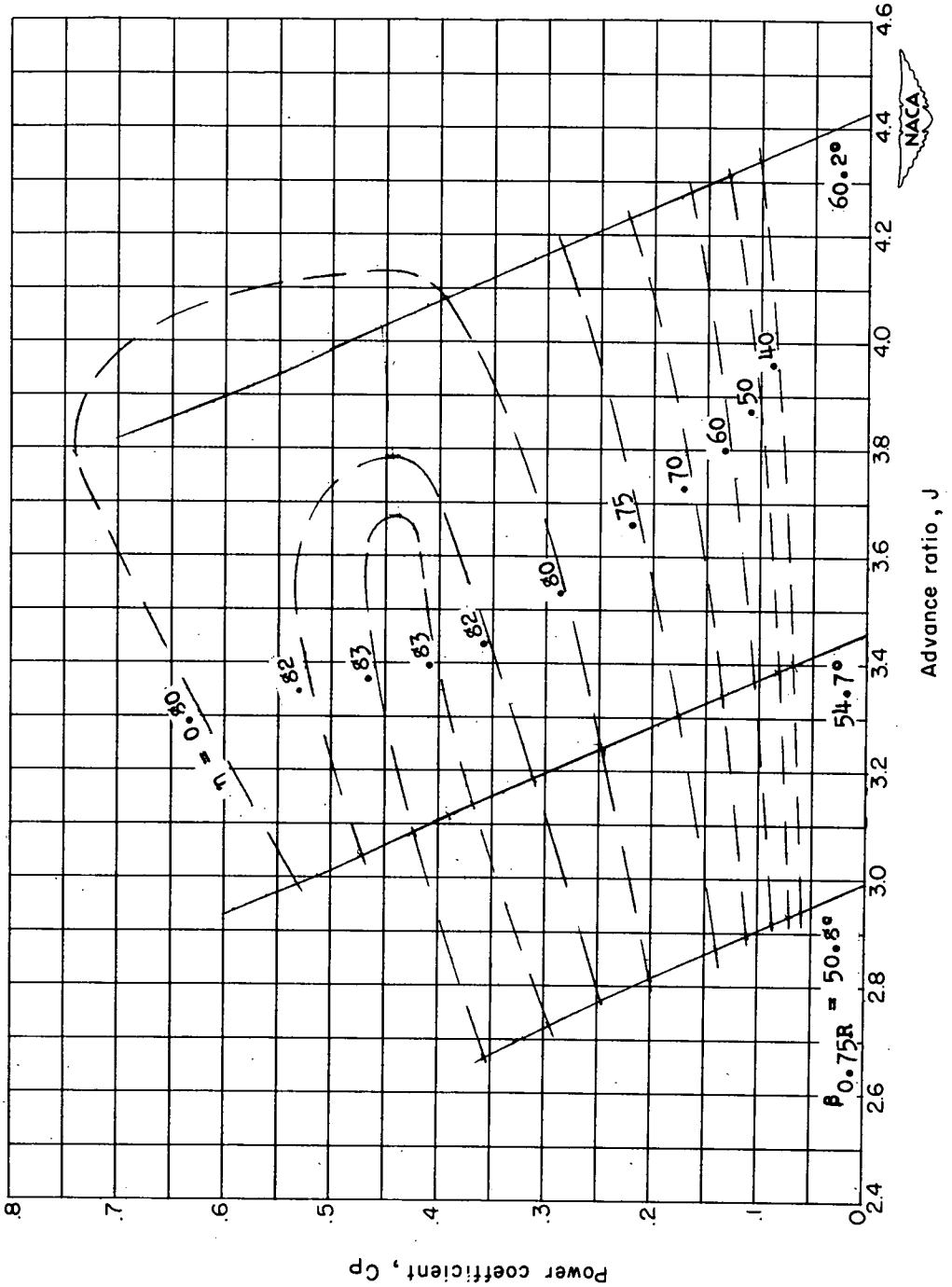

(e) M = 0.80.

Figure 19.- Continued.

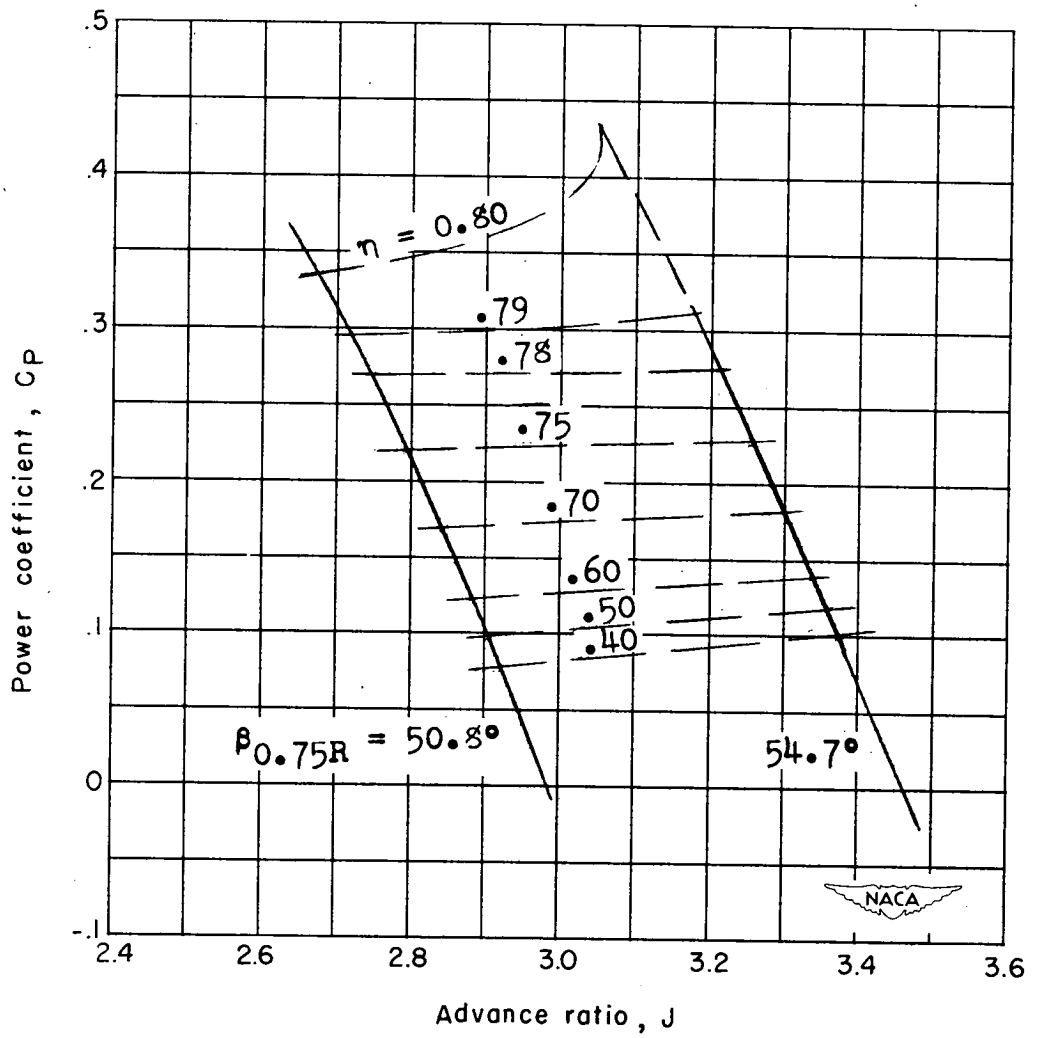

(f) M = 0.84.

Figure 19.- Continued.

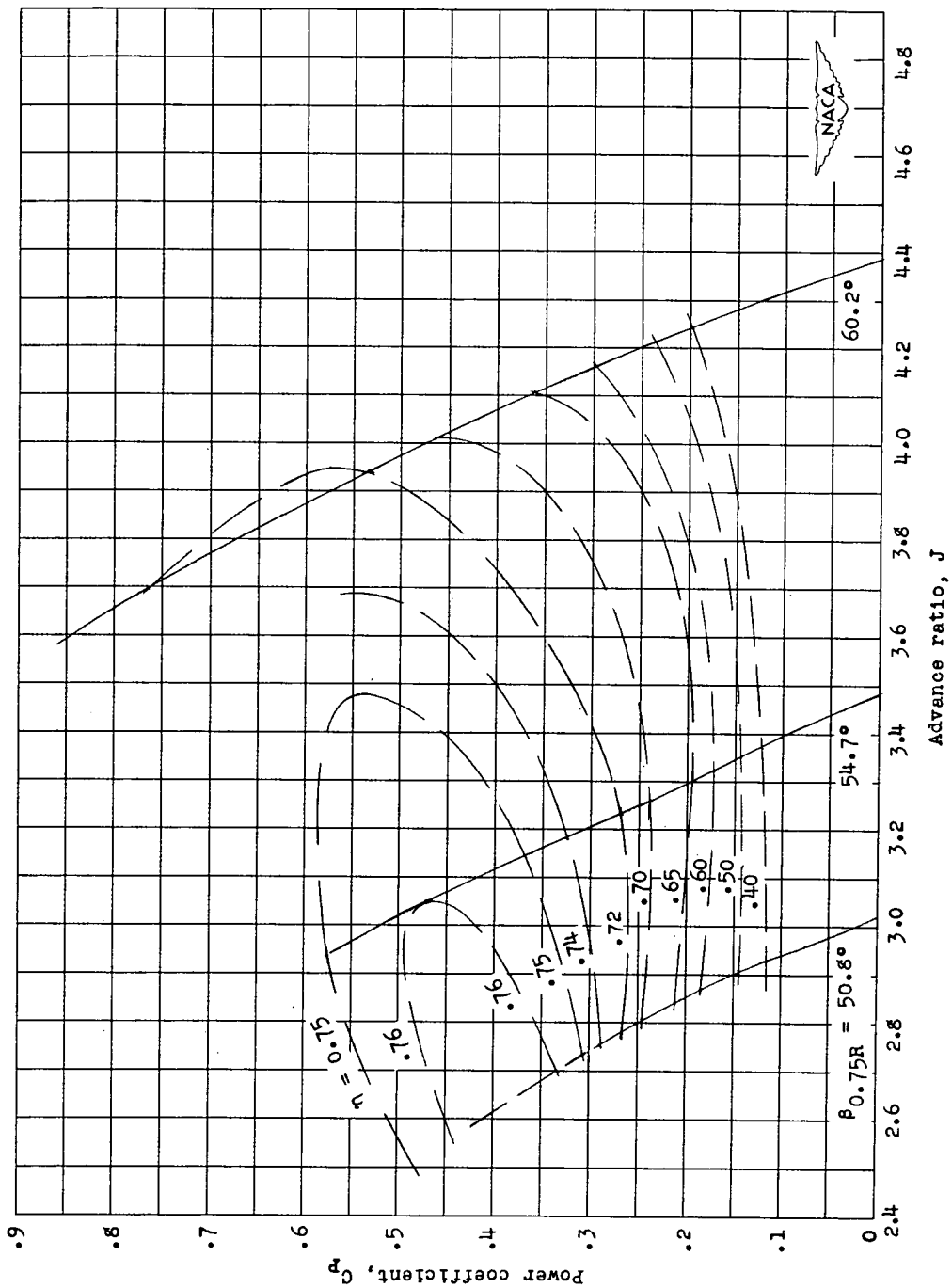

(g) M = 0.89.

Figure 19.- Continued.

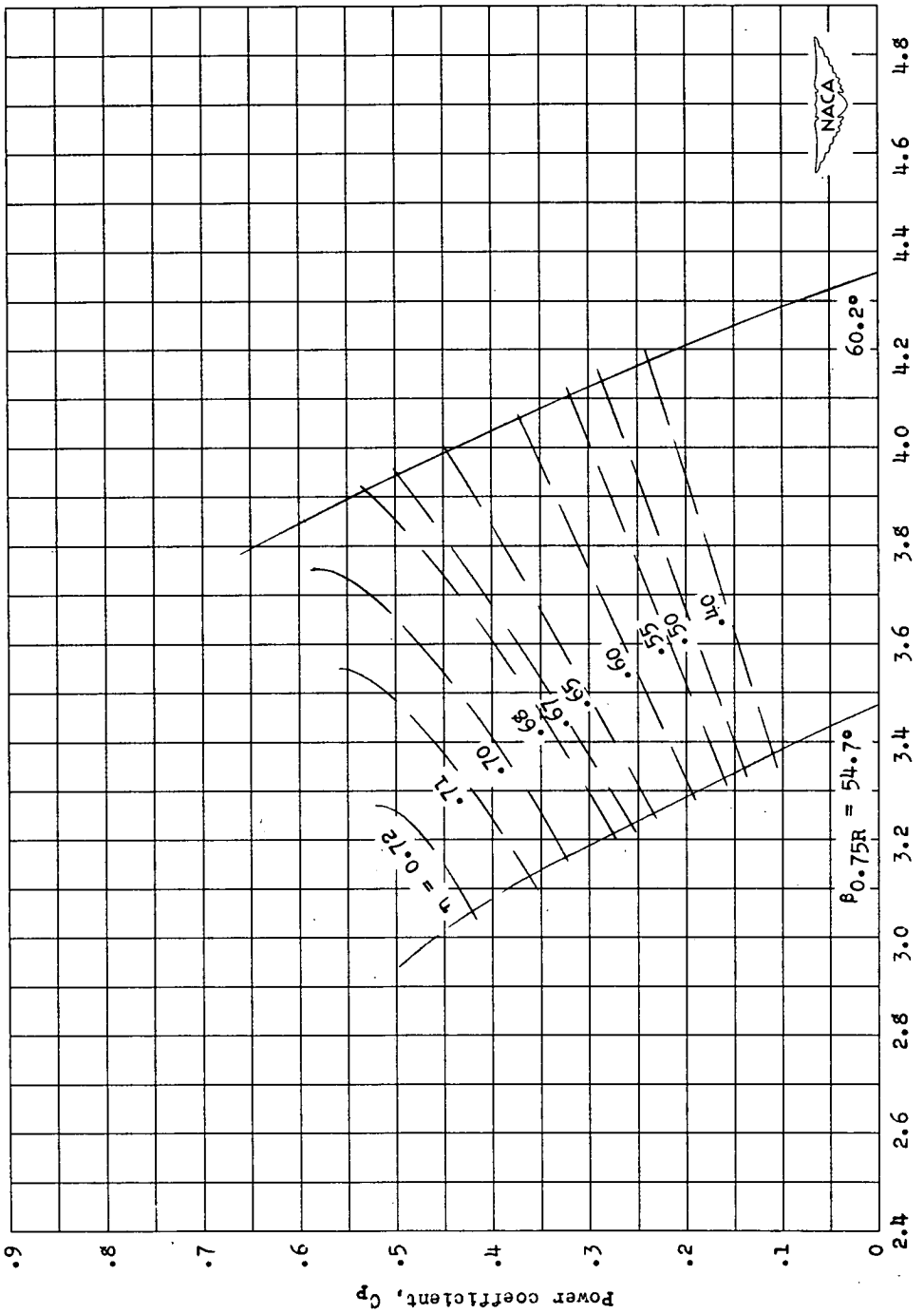

(h) M = 0.93.

Figure 19.- Continued.

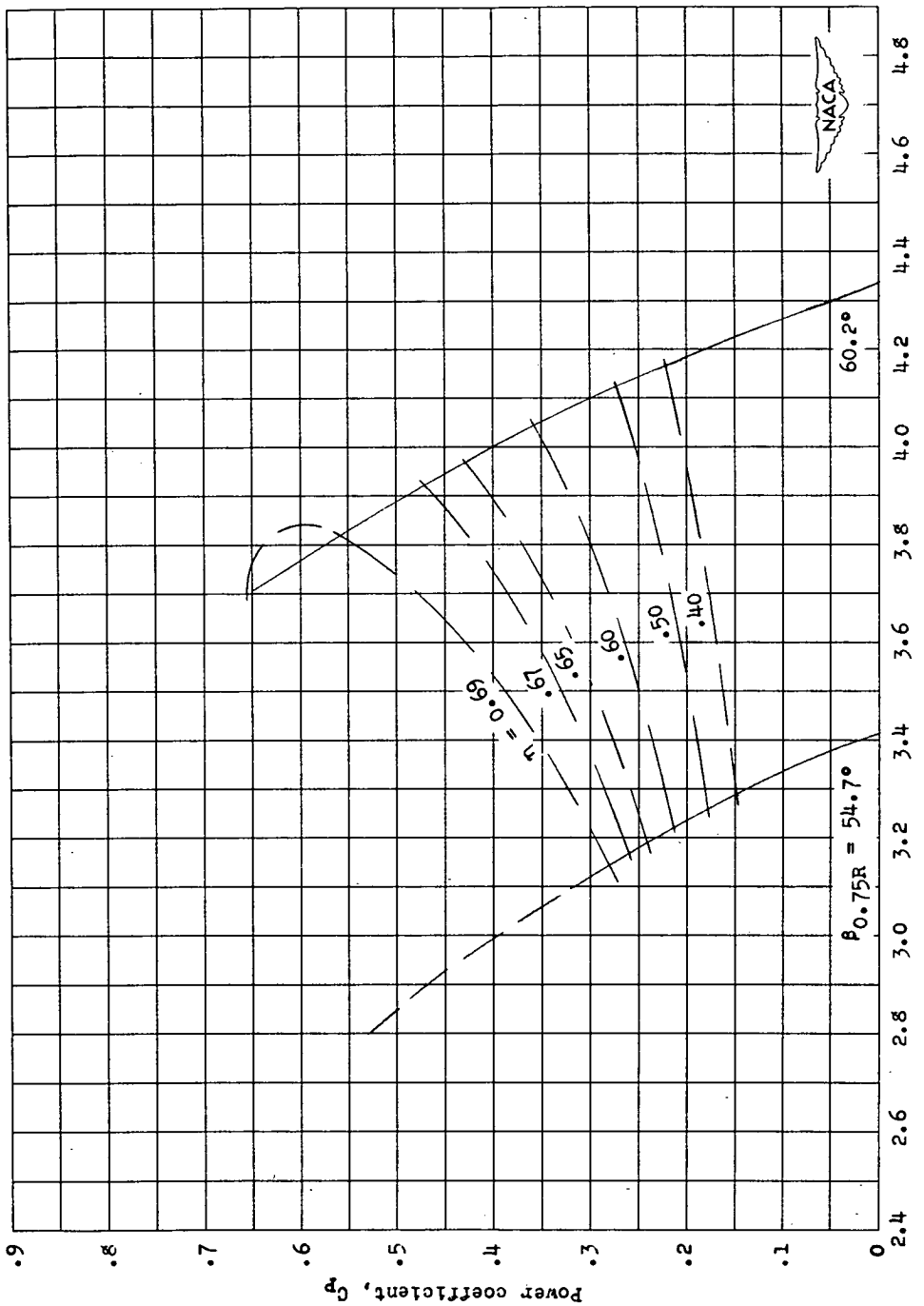

(i) M = 0.96.

Figure 19.- Concluded.

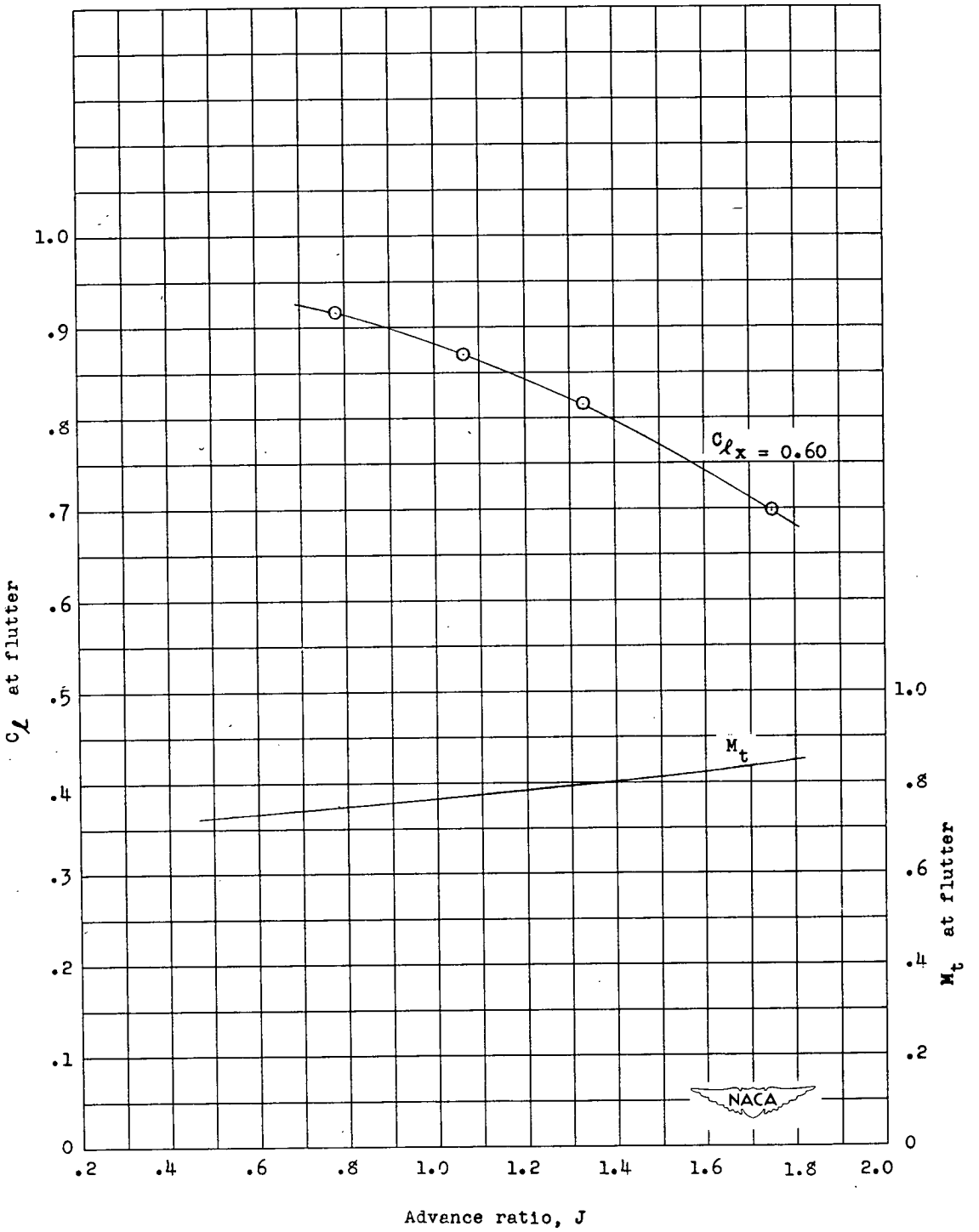

Figure 20.- Variation of lift coefficient and tip Mach number at flutter with advance ratio. x = 0.60; 1600 rpm.

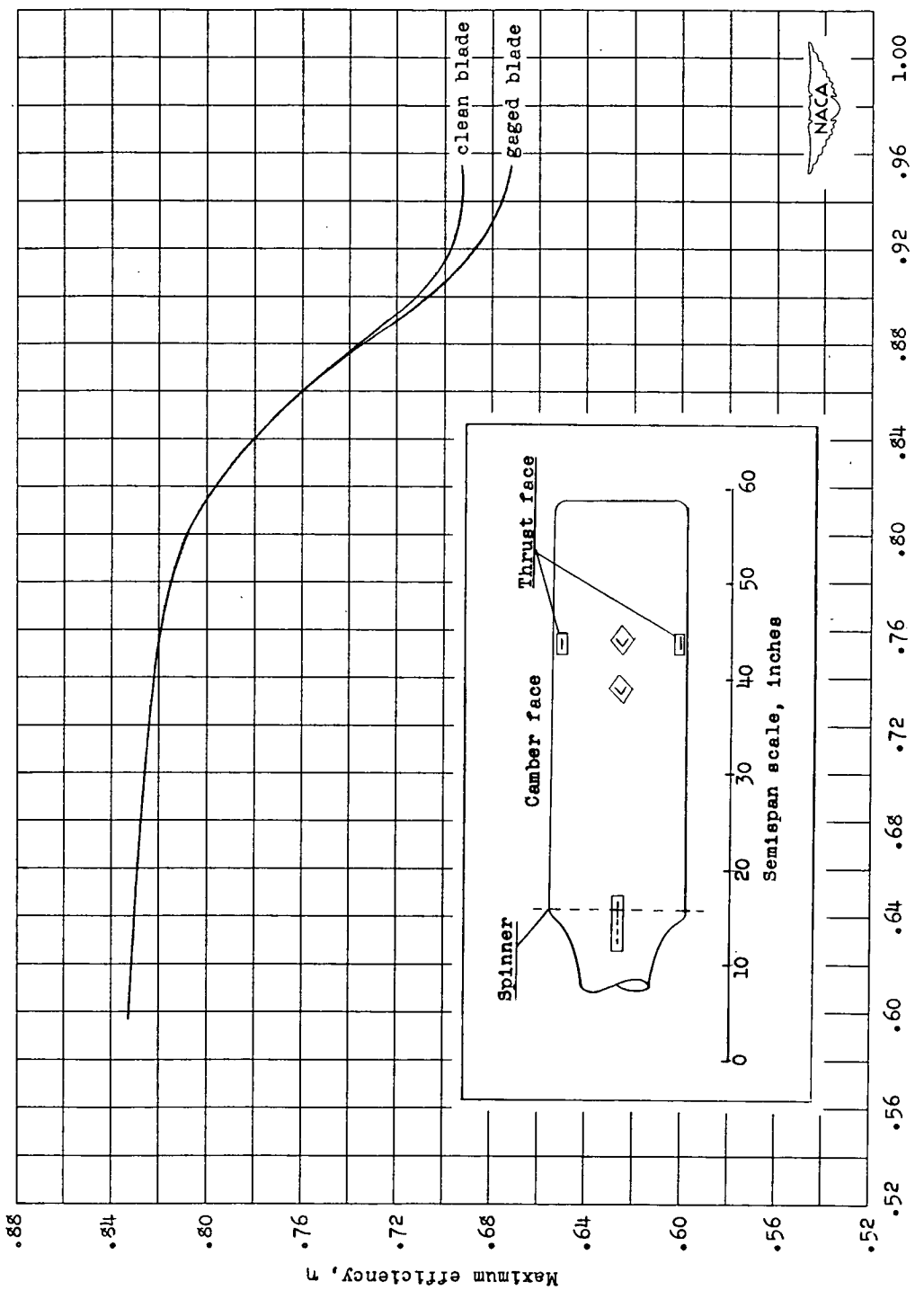

Figure 21.- Effect of strain gages on maximum efficiency.

NACA-Langley - 7-30-53 - 300